an important role in the regulation of synaptic NE concentration in the SA node. Microdialysis is a powerful tool to assess the changes of synaptic NE concentration in the SA node.

Acknowledgements

References

Akiyama, T., Yamazaki, T., Ninomiya, I., 1991. In vivo monitoring of myocardial interstitial norepinephrine by dialysis technique. Am. J. Physiol. 261, H1643–H1647.

Endoh, M., 1975. Effects of dopamine on sinus rate and ventricular contractile force of the dog heart in vitro and in vivo. Br. J. Pharmacol. 55, 475–486.

Glantz, S.A., 2005. Primer of Biostatistics, 6th ed. McGraw-Hill, New York.

Goldstein, D.S., Brush Jr., J.E., Eisenhofer, G., Stull, R., Esler, M., 1988. In vivo measurement of neuronal uptake of norepinephrine in the human heart. Circulation 78, 41–48.

Kawada, T., Miyamoto, T., Uemura, K., Kashihara, K., Kamiya, A., Sugimachi, M., Sunagawa, K., 2004. Effects of neuronal norepinephrine uptake blockade on baroreflex neural and peripheral arc transfer characteristics. Am. J. Physiol. Regul. Integr. Comp. Physiol. 286, R1110–R1120.

Meredith, I.T., Eisenhofer, G., Lambert, G.W., Dewar, E.M., Jennings, G.L., Esler, M.D., 1993. Cardiac sympathetic nervous activity in congestive heart failure. Evidence for increased neuronal norepinephrine release and preserved neuronal uptake. Circulation 88, 136–145.

Shimizu, S., Akiyama, T., Kawada, T., Shishido, T., Yamazaki, T., Kamiya, A., Mizuno, M., Sano, S., Sugimachi, M., 2009. In vivo direct monitoring of vagal acetylcholine release to the sinoatrial node. Auton. Neurosci. 148, 44–49.

Toda, N., 1969. Interactions of ouabain and noradrenaline in isolated rabbit's atria. Br. J. Pharmacol. 36, 393–408.

ARTICLE IN PRESS

Contents lists available at ScienceDirect

Neurochemistry International
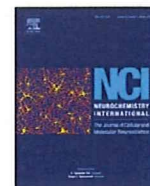
Role of Ca^{2+}-activated K^+ channels in catecholamine release from *in vivo* rat adrenal medulla

Tsuyoshi Akiyama [a,*], Toji Yamazaki [a], Toru Kawada [b], Shuji Shimizu [b], Masaru Sugimachi [b], Mikiyasu Shirai [a]

[a] Department of Cardiac Physiology, National Cardiovascular Center Research Institute, 5-7-1 Fujishiro-dai, Suita, 565-8565 Osaka, Japan
[b] Department of Cardiovascular Dynamics, National Cardiovascular Center Research Institute, Suita, 565-8565, Japan

ARTICLE INFO

ABSTRACT

To elucidate the role of Ca^{2+}-activated K^+ (K_{Ca}) channels in the presynaptic acetylcholine (ACh) release from splanchnic nerve endings and the postsynaptic catecholamine release from chromaffin cells, we applied microdialysis technique to the left adrenal medulla of anesthetized rats and investigated the effects of local administration of K_{Ca} channel antagonists through dialysis probes on the release of ACh and/or catecholamine, induced by electrical stimulation of splanchnic nerves or local administration of ACh through the dialysis probes. *Nerve stimulation-induced release*: in the presence of a cholinesterase inhibitor, neostigmine, large-conductance K_{Ca} (BK) channel antagonists, iberiotoxin and paxilline enhanced the presynaptic ACh release and postsynaptic norepinephrine (NE) and epinephrine (Epi) release. Small-conductance K_{Ca} (SK) channel antagonists, apamin and scyllatoxin enhanced the Epi release without any changes in ACh or NE release. In the absence of neostigmine, ACh release was not detected. Iberiotoxin and paxilline enhanced NE and Epi release. Apamin and scyllatoxin had no effect on NE or Epi release. *Exogenous ACh-induced release*: iberiotoxin and paxilline enhanced the Epi release, but had no effect on the NE release. Apamin and scyllatoxin enhanced both NE and Epi release. In conclusion, BK channels on splanchnic nerve endings play an inhibitory role in the physiological catecholamine release from adrenal medulla by limiting presynaptic ACh release while SK channels do not. BK channels on Epi-storing cells may play an inhibitory role in nerve stimulation-induced Epi release. SK channels on NE- and Epi-storing cells play a minor role in nerve stimulation-induced catecholamine release.

© 2009 Elsevier Ltd. All rights reserved.

1. Introduction

The physiological release of catecholamine from adrenal medulla is controlled by central sympathetic neurons through splanchnic nerves. Splanchnic nerve endings make synaptic-like contacts with chromaffin cells (Coupland, 1965). Activation of splanchnic nerve endings causes Ca^{2+} influx through voltage-dependent Ca^{2+} channels, which evokes exocytotic acetylcholine (ACh) release. This ACh release activates cholinergic receptors on chromaffin cells, which causes Ca^{2+} influx through voltage-dependent Ca^{2+} channels and evokes exocytotic catecholamine release from chromaffin cells (García et al., 2006).

Ca^{2+}-activated K^+ (K_{Ca}) currents are consistently found at neuronal cells or nerve terminals (Meir et al., 1999). K_{Ca} channels are located in the vicinity of voltage-dependent Ca^{2+} channels and activated by Ca^{2+} influx through voltage-dependent Ca^{2+} channels. Activation of the K_{Ca} channels induces outward efflux of K^+, causes

hyperpolarization of the membrane, and subsequently limits Ca^{2+} entry through voltage-dependent Ca^{2+} channels. Thus, K_{Ca} channels may be present at two different sites in the adrenal medulla: splanchnic nerve endings and chromaffin cells, and are then involved in the physiological regulation of presynaptic ACh release and/or postsynaptic catecholamine release. In fact, it has been reported that K_{Ca} channels on chromaffin cells play an important role in catecholamine release (Montiel et al., 1995; Uceda et al., 1992; Wada et al., 1995). Little information is, however, available on the role of K_{Ca} channels in the presynaptic ACh release from splanchnic nerve endings.

We have recently developed a dialysis technique to simultaneously monitor the release of presynaptic ACh and postsynaptic catecholamine in the *in vivo* adrenal medulla (Akiyama et al., 2004a). This method makes it possible to investigate the functional roles of K_{Ca} channels in the ACh release from splanchnic nerve endings and the catecholamine release from adrenal medulla in the *in vivo* state. In the present study, we applied the microdialysis technique to the adrenal medulla of anesthetized rats and investigated the effects of K_{Ca} channel antagonists on the release of presynaptic ACh and postsynaptic catecholamine.

* Corresponding author. Tel.: +81 6 6833 5012x2380; fax: +81 6 6872 8092.
E-mail address: takiyama@ri.ncvc.go.jp (T. Akiyama).

In electrophysiological studies, K_{Ca} channels can be divided into two types based on their single channel conductance: large-conductance (BK) and small-conductance K_{Ca} (SK) channels (Blatz and Magleby, 1987). We tested two types of BK channel antagonists: the selective peptidergic BK channel antagonist, iberiotoxin (Candia et al., 1992) and the non-peptidergic BK channel antagonist, paxilline (Kanus et al., 1994). Similarly we tested two types of SK channel antagonists: the selective peptidergic SK channel antagonist, apamin (Blatz and Magleby, 1986) and the selective peptidergic SK channel antagonist different in amino acid sequence, scyllatoxin (Auguste et al., 1990).

2. Materials and methods

2.1. Animal preparation

Animal care was provided in strict accordance with the *Guiding Principles for the Care and Use of Animals in the Field of Physiological Sciences* approved by the Physiological Society of Japan. All protocols were approved by the Animal Subject Committee of the National Cardiovascular Center. Adult male Wistar rats weighing 380–460 g were anesthetized with pentobarbital sodium (50–55 mg/kg, i.p.). A cervical midline incision was made to expose the trachea, which was then cannulated. The rats were ventilated with a constant-volume respirator using room air mixed with oxygen. The left femoral artery and vein were cannulated for monitoring arterial blood pressure and administration of anesthetic, respectively. The level of anesthesia was maintained with a continuous intravenous infusion of pentobarbital sodium (15–25 mg/kg/h, i.v.). The electrocardiogram was monitored to record the heart rate. A thermostatic heating pad was used to keep the esophageal temperature within a range of 37–38 °C. With the animal in the lateral position, the left adrenal gland and left splanchnic nerve were exposed by a subcostal flank incision, and the left splanchnic nerve was transected. In protocols requiring nerve stimulation, shielded bipolar stainless steel electrodes were applied to the distal end of the nerve, which was then stimulated with a digital stimulator (SEN-7203, Nihon Kohden, Japan) with a rectangular pulse (10 V and 1 ms in duration).

2.2. Dialysis technique

Dialysis probe construction was the same as that used in our previous dialysis experiments (Akiyama et al., 2003, 2004a,b). Each end of a dialysis fiber (0.32 mm OD, and 0.25 mm ID; PAN-DX 100,000 mol wt 100% cutoff, Asahi Chemical, Japan) was inserted into a polyethylene tube (25 cm length, 0.5 mm OD, and 0.2 mm ID; SP-8) and glued. The length of the dialysis fiber exposed was 3 mm. At a perfusion speed of 10 μl/min, *in vitro* recovery rates of ACh, norepinephrine (NE) and epinephrine (Epi) were (%): 3.21 ± 0.07, 2.68 ± 0.03, and 2.80 ± 0.03, respectively (number of dialysis probes: 3).

The left adrenal gland was gently lifted, and the dialysis probe was implanted in the medulla of the left adrenal gland along the long axis using a fine guiding needle. The dialysis probe was perfused with Ringer's solution or Ringer's solution containing pharmacological agents at a speed of 10 μl/min using a microinjection pump (CMA/100, Carnegie Medicin, Sweden). Ringer's solution consisted of (in mM) 147.0 NaCl, 4.0 KCl, 2.25 $CaCl_2$. All K_{Ca} channel antagonists tested were locally administered by perfusion through the dialysis probe after being dissolved in Ringer's solution. We started the protocols followed by a stabilization period of 3–4 h and sampled dialysate taking the dead space volume between the dialysis membrane and sample tube into account. Dialysate ACh and catecholamine concentrations were separately measured using each high-performance liquid chromatography with electrochemical detection as previously described (Akiyama et al., 2004a,b).

2.3. Experimental protocols

The experiment was performed based on the previous experiment showing that dialysate ACh and/or catecholamine responses were reproducible on repetition of the pharmacological or electrical stimulation (Akiyama et al., 2004a,b). At the end of the experiment, the rats were sacrificed with pentobarbital sodium, and the implant sites were examined. The dialysis probes were confirmed to have been implanted in the adrenal medulla, and no bleeding or necrosis was found macroscopically.

2.4. Protocol 1

We perfused the dialysis probe with Ringer's solution containing a cholinesterase inhibitor, neostigmine (10 μM) and investigated the effects of BK and SK channel antagonists on the nerve stimulation-induced responses of dialysate ACh and catecholamine concentration. The left splanchnic nerves were firstly electrically stimulated for 2 min at 2 Hz. Then, after a 30-min interval, nerves were subjected to a second stimulation for 2 min at 4 Hz. After these control

stimulations, local administration of iberiotoxin (1 μM, $n = 7$), paxilline (100 μM, $n = 7$), apamin (10 μM, $n = 7$) or scyllatoxin (2 μM, $n = 7$) was started. Thirty minutes after local administration of K_{Ca} channel antagonists, nerves were stimulated for 2 min at 2 Hz. Next, after a 30-min interval, nerves were stimulated again for 2 min at 4 Hz. Phosphate buffer (pH 3.5, 4 μl) was transferred into each sample tube before dialysate sampling. Two dialysate samples were continuously collected per nerve stimulation: one before and one during stimulation. One sampling period was 2 min (1 sample volume = 20 μl). Half of the dialysate sample was used for the measurement of ACh, and the remaining half for the measurement of NE and Epi.

2.5. Protocol 2

We investigated the effects of K_{Ca} channel antagonists on the nerve stimulation-induced catecholamine release in the absence of neostigmine. Like in protocol 1, the left splanchnic nerves were stimulated before and 30 min after administration of iberiotoxin ($n = 7$), paxilline ($n = 7$), apamin ($n = 7$) or scyllatoxin ($n = 7$) and two dialysate samples were collected per nerve stimulation. The dialysate sample was used for the measurement of NE and Epi.

2.6. Protocol 3

We investigated the effects of K_{Ca} channel antagonists on exogenous ACh-induced catecholamine release. The dialysis probe was perfused with Ringer's solution. ACh (1 mM) was locally administered to the adrenal medulla through the dialysis probe for 1 min. After first administration of ACh, local administration of iberiotoxin (1 μM, $n = 7$), paxilline (100 μM, $n = 7$), apamin (10 μM, $n = 7$) or scyllatoxin (2 μM, $n = 7$) was started. Thirty minutes after local administration of K_{Ca} channel antagonists, ACh (1 mM) was locally administered again for 1 min. Phosphate buffer (pH 3.5, 2 μl) was transferred into each sample tube before dialysate sampling. Two dialysate samples were continuously collected per local administration of ACh: one before and one during administration. One sampling period was 1 min (1 sample volume = 10 μl). The dialysate sample was used for the measurement of NE and Epi.

2.7. Drugs

Drugs were mixed fresh for each experiment. Neostigmine methylsulfate (Shionogi, Japan), iberiotoxin (Peptide Institute, Japan), apamin (Peptide Institute) and scyllatoxin (Peptide Institute) were dissolved and diluted in Ringer's solution. Paxilline (Sigma Chemical, USA) was dissolved in DMSO and diluted in Ringer's solution. The final concentration of DMSO in the working solution was 0.5% (v/v).

2.8. Statistical methods

To examine the effects of nerve stimulation, local administration of ACh, and K_{Ca} channel antagonists, we analyzed heart rate and mean arterial pressure, basal dialysate NE and Epi content, and dialysate ACh, NE and Epi responses, by using one-way analysis of variance with repeated measures. When statistical significance was detected, the Newman–Keuls test was applied (Winer, 1971). Statistical significance was defined as $P < 0.05$. Values are presented as means $\pm$ SE.

3. Results

3.1. Changes in heart rate and mean arterial pressure

Local administration of neostigmine, K_{Ca} channel antagonists, and ACh through the dialysis probe did not change basal heart rate or mean arterial pressure. In protocol 1, nerve stimulation increased mean arterial pressure from 113 ± 3 mmHg in control to 131 ± 2 mmHg at 2 Hz ($n = 28$, $P < 0.05$) and 132 ± 2 mmHg at 4 Hz ($n = 28$, $P < 0.05$), and decreased heart rate from 436 ± 4 beats/min in control to 424 ± 4 beats/min at 2 Hz ($n = 28$, $P < 0.05$) and 420 ± 4 beats/min at 4 Hz ($n = 28$, $P < 0.05$). In protocol 2, nerve stimulation increased mean arterial pressure from 115 ± 4 mmHg in control to 129 ± 3 mmHg at 2 Hz ($n = 28$, $P < 0.05$) and 131 ± 3 mmHg at 4 Hz ($n = 28$, $P < 0.05$), and decreased heart rate from 423 ± 3 beats/min in control to 410 ± 4 beats/min at 2 Hz ($n = 28$, $P < 0.05$) and 404 ± 3 beats/min at 4 Hz ($n = 28$, $P < 0.05$). Heart rate and mean arterial pressure recovered to basal levels after nerve stimulation. After administration of K_{Ca} channel antagonists, nerve stimulation evoked the same responses of heart rate and mean arterial pressure.

Table 1
Basal NE and Epi release before and after local administration of K_{Ca} channel antagonists.

	NE (nM)	Epi (nM)
Iberiotoxin ($n = 21$)		
Before administration	4.8 ± 0.3	16.7 ± 1.0
After administration	5.0 ± 0.4	$21.7 \pm 1.6^*$
Paxilline ($n = 21$)		
Before administration	4.7 ± 0.3	15.7 ± 1.1
After administration	4.8 ± 0.4	$22.0 \pm 1.9^*$
Apamin ($n = 21$)		
Before administration	4.9 ± 0.4	17.1 ± 1.1
After administration	4.6 ± 0.5	$21.2 \pm 1.6^*$
Scyllatoxin ($n = 21$)		
Before administration	4.9 ± 0.3	15.3 ± 0.7
After administration	5.1 ± 0.4	$20.6 \pm 0.9^*$

Values are means $\pm$ SE. n, no. of rats; NE, norepinephrine; Epi, epinephrine. $^*P < 0.05$ vs. values before administration.

3.2. Basal ACh and catecholamine release

ACh could not be detected in dialysate before nerve stimulation even in the presence of neostigmine. In contrast, substantial amounts of NE and Epi were observed in dialysate before nerve stimulation or ACh administration. Local administration of neostigmine did not influence this basal catecholamine release. BK channel antagonists, iberiotoxin and paxilline did not change basal NE release but increased basal Epi release. Similarly, the SK channel antagonists, apamin and scyllatoxin did not change basal NE release, but increased basal Epi release (Table 1).

ACh was detected in dialysate only during nerve stimulation in the presence of neostigmine. Thus, we expressed this detected dialysate ACh concentration as an index of ACh release induced by nerve stimulation. In contrast, we subtracted basal dialysate NE and Epi content before nerve stimulation or ACh administration from those during stimulation or ACh administration, and expressed these subtracted values as indices of NE and Epi release induced by nerve stimulation or ACh administration.

3.3. Effects of K_{Ca} channel antagonists on the nerve stimulation-induced ACh and catecholamine release in the presence of neostigmine

Iberiotoxin enhanced the nerve stimulation-induced release of presynaptic ACh and postsynaptic catecholamine (Fig. 1A). ACh release increased from 4.5 ± 0.8 to 7.4 ± 0.7 nM at 2 Hz and from 9.4 ± 1.0 to 14.0 ± 1.0 nM at 4 Hz. NE release increased from 7 ± 0.5 to 32 ± 3 nM at 2 Hz and from 27 ± 3 to 74 ± 9 nM at 4 Hz. Epi release increased from 39 ± 5 to 78 ± 5 nM at 2 Hz, and from 105 ± 8 to 193 ± 15 nM at 4 Hz. Similarly, paxilline enhanced the nerve stimulation-induced release of ACh and catecholamine (Fig. 1B). ACh release increased from 4.1 ± 0.4 to 5.9 ± 0.5 nM at 2 Hz and from 9.4 ± 0.7 to 13.7 ± 0.9 nM at 4 Hz. NE release increased from 11 ± 2 to 26 ± 4 nM at 2 Hz, from 31 ± 5 to 58 ± 8 nM at 4 Hz. Epi release increased from 41 ± 7 to 77 ± 14 nM at 2 Hz and from 108 ± 14 to 195 ± 17 nM at 4 Hz.

Apamin had no effect on the nerve stimulation-induced release of ACh and NE, but enhanced the nerve stimulation-induced Epi release (Fig. 2A). Epi release increased from 45 ± 3 to 59 ± 4 nM at 2 Hz and from 108 ± 7 to 139 ± 17 nM at 4 Hz. Scyllatoxin had no effect on the nerve stimulation-induced release of ACh and NE either, but enhanced the nerve stimulation-induced Epi release (Fig. 2B). Epi release increased from 37 ± 4 to 50 ± 3 nM at 2 Hz and from 122 ± 5 to 152 ± 12 nM at 4 Hz.
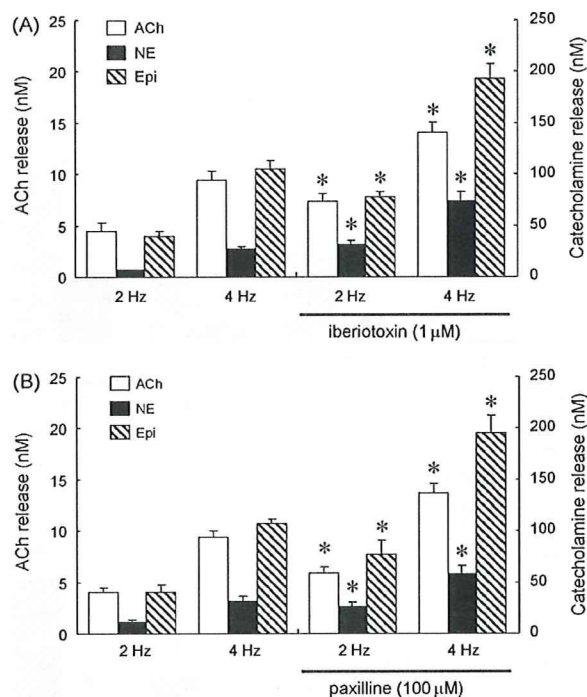
Fig. 1. Effects of BK channel antagonists on the nerve stimulation-induced release of acetylcholine (ACh), norepinephrine (NE) and epinephrine (Epi) in the presence of neostigmine (10 μM): iberiotoxin (A) and paxilline (B) enhanced the release of ACh, NE and Epi at 2 and 4 Hz. Values are means $\pm$ SE from seven rats. $^*P < 0.05$ vs. ACh, NE or Epi release at the same frequency as before administration of BK channel antagonists.
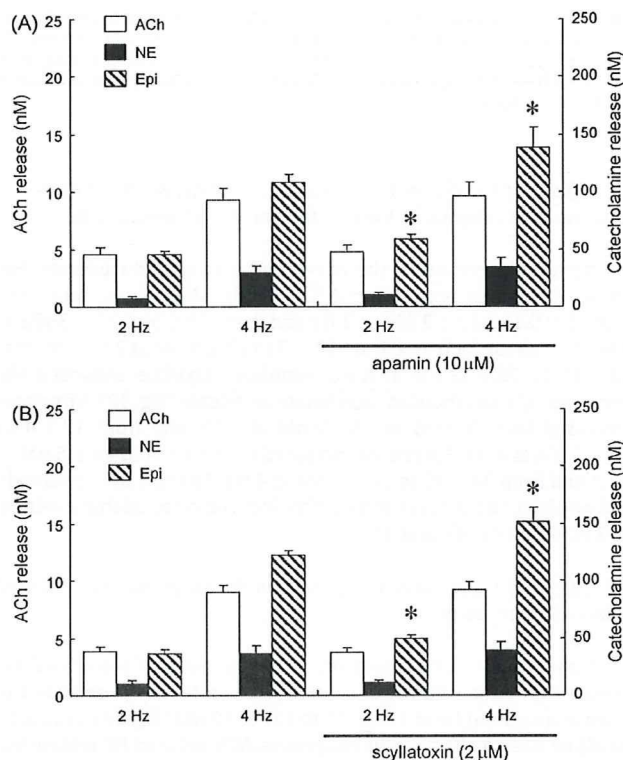
Fig. 2. Effects of SK channel antagonists on the nerve stimulation-induced release of ACh, NE and Epi in the presence of neostigmine (10 μM): apamin (A) and scyllatoxin (B) had no effect on the release of ACh or NE, but enhanced the Epi release at 2 and 4 Hz. Values are means $\pm$ SE from seven rats. $^*P < 0.05$ vs. ACh, NE or Epi release at the same frequency as before administration of SK channel antagonists.

4
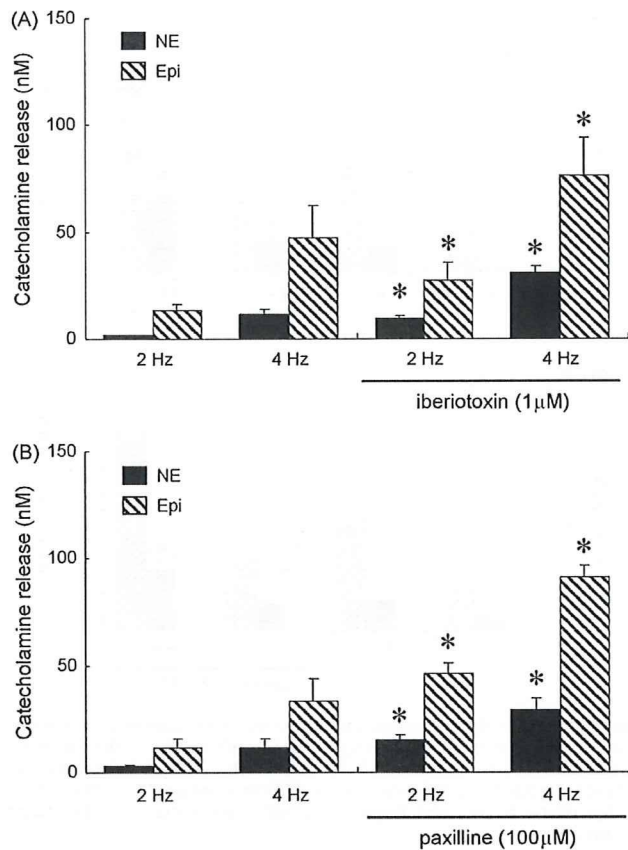
Fig. 3. Effects of BK channel antagonists on the nerve stimulation-induced release of NE and Epi in the absence of neostigmine: iberiotoxin (A) and paxilline (B) enhanced the release of NE and Epi at 2 and 4 Hz. Values are means ± SE from seven rats. *$P < 0.05$ vs. NE or Epi release at the same frequency as before administration of BK channel antagonists.

Fig. 4. Effects of SK channel antagonists on the nerve stimulation-induced release of NE and Epi in the absence of neostigmine: apamin (A) and scyllatoxin (B) had no effect on the release of NE or Epi at 2 or 4 Hz. Values are means ± SE from seven rats.

3.4. Effects of K_{Ca} channel antagonists on the nerve stimulation-induced catecholamine release in the absence of neostigmine

Iberiotoxin enhanced the nerve stimulation-induced catecholamine release at both 2 and 4 Hz (Fig. 3A). NE release increased from 2 ± 0.3 to 10 ± 2 nM at 2 Hz and from 12 ± 3 to 31 ± 3 nM at 4 Hz. Epi release increased from 13 ± 3 to 27 ± 9 nM at 2 Hz and from 47 ± 15 to 76 ± 18 nM at 4 Hz. Similarly, paxilline enhanced the nerve stimulation-induced catecholamine release (Fig. 3B). NE release increased 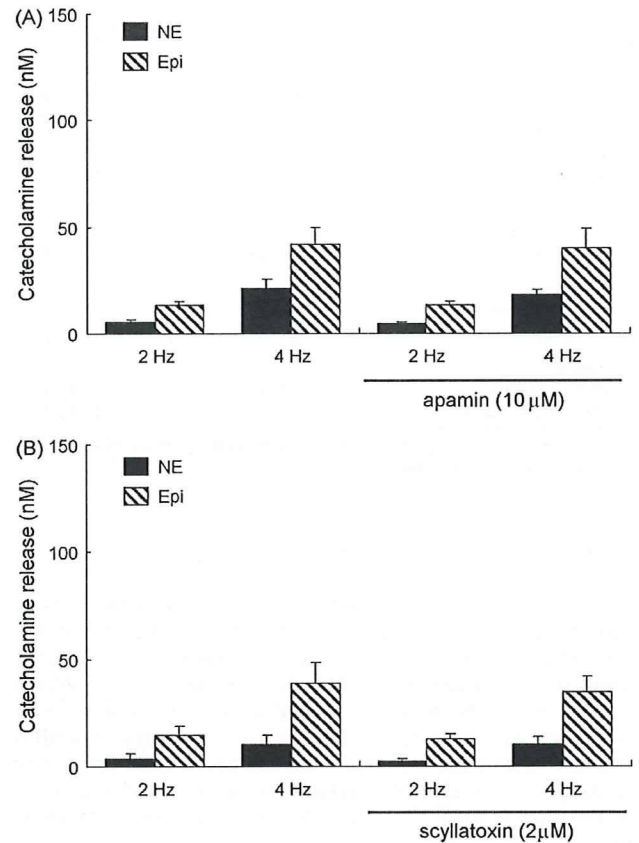from 3 ± 0.6 to 15 ± 2 nM at 2 Hz and from 12 ± 4 to 29 ± 5 nM at 4 Hz. Epi release increased from 12 ± 4 to 46 ± 5 nM at 2 Hz and from 34 ± 10 to 91 ± 6 nM at 4 Hz. Apamin and scyllatoxin had no effect on the nerve stimulation-induced catecholamine release at 2 or 4 Hz (Fig. 4A and B).

3.5. Effects of K_{Ca} channel antagonists on the exogenous ACh-induced catecholamine release

Iberiotoxin had no effect on the exogenous ACh-induced NE release, but enhanced the exogenous ACh-induced Epi release. Epi release increased from 108 ± 11 to 127 ± 10 nM (Fig. 5A). Similarly, paxilline had no effect on the exogenous ACh-induced NE release but enhanced the exogenous ACh-induced Epi release. Epi release increased from 93 ± 5 to 137 ± 13 nM (Fig. 5B). Apamin enhanced the exogenous ACh-induced catecholamine release (Fig. 6A). NE release increased from 37 ± 4 to 49 ± 4 nM and Epi release from 103 ± 8 to 122 ± 9 nM. Similarly scyllatoxin enhanced the

exogenous ACh-induced catecholamine release (Fig. 6B). NE release increased from 32 ± 3 to 47 ± 3 nM and Epi release from 108 ± 6 to 140 ± 11 nM.

4. Discussion

4.1. Roles of K_{Ca} channels on splanchnic nerve endings in presynaptic ACh release

We found that, in the in vivo adrenal medulla, both iberiotoxin and paxilline enhanced the nerve stimulation-induced release of presynaptic ACh at 2 and 4 Hz by ~50% in the presence of neostigmine (Fig. 1). BK channels currents have been confirmed on cholinergic nerve endings including motor nerves in the neuromuscular junction (Flink and Atchison, 2003), presynaptic nerves in the chick ciliary ganglion (Sun et al., 1999) and tracheal parasympathetic nerves (Zhang et al., 1998). Activation of the K_{Ca} conductance is considered to limit Ca^{2+} entry through voltage-dependent Ca^{2+} channels, and subsequently reduce transmitter release (Meir et al., 1999). Our results strongly suggest that BK channels are present on the splanchnic nerve endings and involved in the control of ACh release. In the perfused cat adrenal gland, charybdotoxin, a BK channel antagonist, enhanced catecholamine release when transmural electrical stimulation was applied at low external Ca^{2+} concentrations, but not when exogenous ACh was administered (Montiel et al., 1995). In the perfused rat adrenal gland, charybdotoxin enhanced the release of Epi and NE induced by transmural electrical stimulation, but not the release induced by administration of ACh (Nagayama et al., 2000b). These indirect studies suggested that BK channels may be involved in the control
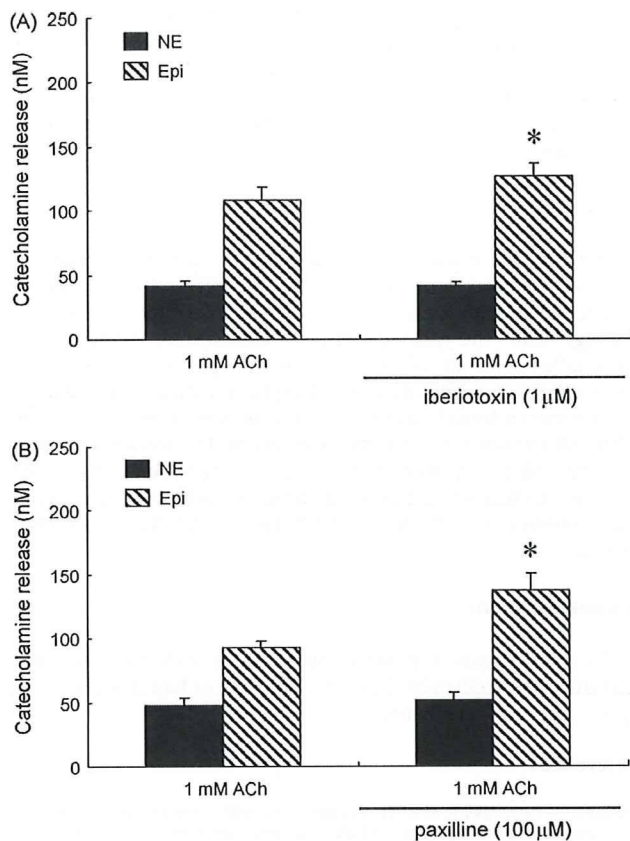
Fig. 5. Effects of BK channel antagonists on the exogenous ACh-induced release of NE and Epi: iberiotoxin (A) and paxilline (B) had no effect on NE release, but enhanced Epi release. Values are means ± SE from seven rats. *$P < 0.05$ vs. NE or Epi release before administration of BK channel antagonists.
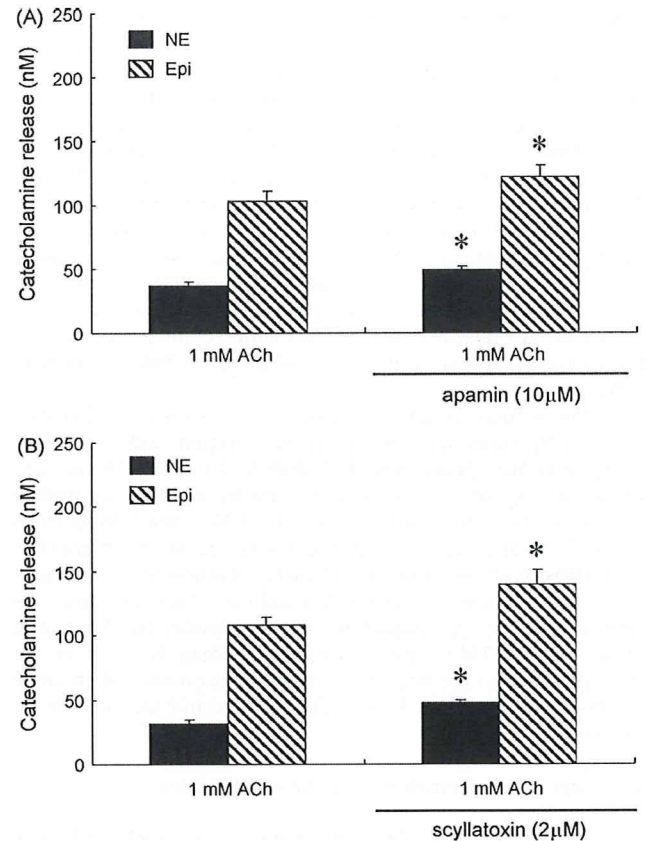
Fig. 6. Effects of SK channel antagonists on the exogenous ACh-induced release of NE and Epi: apamin (A) and scyllatoxin (B) enhanced the release of NE and Epi. Values are means ± SE from seven rats. *$P < 0.05$ vs. NE or Epi release before administration of SK channel antagonists.

of catecholamine release at the presynaptic site. But there has been no direct study investigating the effect of BK channel antagonists on ACh release from splanchnic nerve endings. This is the first direct study to demonstrate that BK channels are involved in the control of ACh release from splanchnic nerve endings. In the *in vivo* adrenal medulla, we observed a substantial enhancement of ACh release by BK channel antagonists at a frequency of 2 Hz with this degree of enhancement being similar to that at a frequency of 4 Hz (Fig. 1). BK channels on splanchnic nerve endings could be functional under physiological conditions. In our previous study, the nerve stimulation-induced catecholamine release was in large part cholinergic in the presence or absence of neostigmine (Akiyama et al., 2003). Thus, BK channels play an inhibitory role in the physiological catecholamine release from adrenal medulla by limiting presynaptic ACh release.

In contrast to BK channel antagonists, apamin and scyllatoxin had no effect on the nerve stimulation-induced ACh release at 2 or 4 Hz (Fig. 2). In perfused cat adrenal glands preloaded with [³H]-choline, apamin did not modify the efflux of [³H]-labeled compound evoked by transmural electrical stimulation (Montiel et al., 1995). SK channels seem to be absent on splanchnic nerve endings or play a minor role in the ACh release from splanchnic nerve endings.

4.2. Role of K_{Ca} channels on chromaffin cells in catecholamine release

Iberiotoxin and paxilline had no effect on the exogenous ACh-induced NE release, but enhanced exogenous ACh-induced Epi release (Fig. 5). Adrenal chromaffin cells are divided into two

populations: NE- and Epi-storing cells (Coupland, 1984). While BK channels seem to be absent on NE-storing cells or play a minor role in the nerve stimulation-induced NE release, BK channels seem to be present on Epi-storing cells. It has been reported that BK channels present at rat chromaffin cells are activated by Ca²⁺ influx and contribute to the rapid termination of action potentials (Prakriya and Lingle, 1999), while iberiotoxin augments the nicotinic receptor-mediated catecholamine secretion from bovine adrenal chromaffin cells (Wada et al., 1995). The enhancement by BK channel antagonists of nerve stimulation-induced Epi release may be in part ascribed to their direct effects on Epi-storing cells. BK channels on Epi-storing cells may be involved in the control of nerve stimulation-induced Epi release. In perfused rat and cat adrenal glands, charybdotoxin, a BK channel antagonist, does not affect the exogenous ACh-induced catecholamine release (Montiel et al., 1995; Nagayama et al., 2000b). Our results of Epi release were inconsistent with these studies, possibly due to differences in the BK channel antagonists used and/or in methodology because charybdotoxin is pharmacologically less selective than iberiotoxin for BK channels (Garcia et al., 1991).

Both apamin and scyllatoxin enhanced the nerve stimulation-induced Epi release in the presence of neostigmine without changes in ACh release (Fig. 2), and the exogenous ACh-induced release of NE and Epi (Fig. 6). These results suggest that SK channels are present on both NE- and Epi-storing cells and that such enhancement is due to the direct effects of SK channel antagonists on chromaffin cells. Neither apamin nor scyllatoxin, however, had any effect on the nerve stimulation-induced NE release in the presence or absence of neostigmine, and the nerve

stimulation-induced Epi release in the absence of neostigmine (Figs. 2 and 4). SK channels on chromaffin cells may play a minor role in the nerve stimulation-induced catecholamine release. It has been reported that SK channels on chromaffin cells are activated by muscarinic receptor stimulation (Nagayama et al., 2000a; Uceda et al., 1992). In our previous study of the same preparation, we demonstrated that muscarinic receptors are present on NE- and Epi-storing cells but play a minor role in the nerve stimulation-induced release of NE and Epi, and that cholinesterase inhibitor elicited muscarinic receptor-mediated Epi release when splanchnic nerve was stimulated (Akiyama et al., 2003). Therefore, SK channels on NE- and Epi-storing cells play an important role in the catecholamine release induced by activation of muscarinic or noncholinergic receptors including PACAP receptor (Fukushima et al., 2002).

In the perfused rat adrenal gland, apamin enhanced NE release induced by transmural electrical stimulation and a nicotinic receptor agonist (Nagayama et al., 2000b). Therefore, SK channels on NE-storing cells could be activated by nicotinic as well as muscarinic receptors. But, our results of NE release induced by nerve stimulation were inconsistent with this study. In anesthetized dogs, scyllatoxin enhanced catecholamine release induced by a nicotinic receptor agonist but did not affect catecholamine release induced by splanchnic nerve stimulation (Nagayama et al., 1998). Thus, this inconsistency may be due to the difference in the method of nerve stimulation and SK channels on NE-storing cells may be activated by nicotinic receptors in the extrasynaptic region.

4.3. Roles of K_{Ca} channels in basal NE and Epi release

In the present study, substantial basal release of NE and Epi was observed in dialysate before nerve stimulation or ACh administration. Both BK and SK channel antagonists enhanced the basal Epi release but not the basal NE release. In our preparation, splanchnic nerves had been transected before control sampling and basal catecholamine release was not enhanced by a cholinesterase inhibitor, neostigmine. Furthermore, using the same preparation we demonstrated that basal catecholamine release is resistant to not only cholinergic antagonists, but also N-, P/Q-, and L-type Ca^{2+} channel antagonists (Akiyama et al., 2004b). Basal catecholamine release seems to be non-cholinergic and independent of Ca^{2+} influx through voltage-dependent Ca^{2+} channels. Ca^{2+} release from intracellular Ca^{2+} stores may be involved in this basal catecholamine release. It has been suggested in chromaffin cells that K_{Ca} channels on the cell surface are activated by Ca^{2+} release from intracellular Ca^{2+} stores (Ohta et al., 1998). On Epi-storing cells, BK and SK channels may play a role in the Epi release induced by Ca^{2+} release from intracellular Ca^{2+} stores.

4.4. Methodological considerations

Because previous results suggested that distribution across the dialysis membrane is required (Akiyama et al., 2003, 2004a), we used the K_{Ca} channel antagonists at a concentration 10 times higher than that required for complete channel blockade in experimental settings in vitro. Then, we tested two different types of selective BK and SK channel antagonists in the present study because higher concentrations of K_{Ca} channel antagonists might induce other pharmacological effects.

Cholinesterase inhibitor was necessary to monitor endogenous ACh even during the splanchnic nerve stimulation because released ACh is rapidly degraded by acetylcholinesterase before reaching the dialysis fiber. Then, we examined the effects of K_{Ca} channel antagonists in the presence or absence of neostigmine because neostigmine may influence the effects of

K_{Ca} channel antagonists. Local administration of neostigmine enhanced the nerve stimulation-induced catecholamine release to about 2-fold before and after administration of K_{Ca} channel antagonists (Figs. 1 and 3). This enhancement could be due to the elevation of synaptic ACh levels by inhibition of acetylcholinesterase.

5. Conclusion

We applied dialysis technique to the adrenal medulla of anesthetized rats and investigated the effects of K_{Ca} channel antagonists on the presynaptic ACh release from splanchnic nerve endings and the postsynaptic catecholamine release from chromaffin cells. BK channels on presynaptic splanchnic nerve endings play an inhibitory role in the physiological catecholamine release from adrenal medulla by limiting presynaptic ACh release while SK channels do not. BK channels on Epi-storing cells may play an inhibitory role in the nerve stimulation-induced Epi release. SK channels are present on NE- and Epi-storing cells, but play a minor role in the nerve stimulation-induced catecholamine release.

Acknowledgment

References

Akiyama, T., Yamazaki, T., Mori, H., Sunagawa, K., 2003. Inhibition of cholinesterase elicits muscarinic receptor-mediated synaptic transmission in the rat adrenal medulla. Auton. Neurosci. 107, 65–73.
Akiyama, T., Yamazaki, T., Mori, H., Sunagawa, K., 2004a. Simultaneous monitoring of acetylcholine and catecholamine release in the in vivo rat adrenal medulla. Neurochem. Int. 44, 497–503.
Akiyama, T., Yamazaki, T., Mori, H., Sunagawa, K., 2004b. Effects of Ca^{2+} channel antagonists on acetylcholine and catecholamine releases in the in vivo rat adrenal medulla. Am. J. Physiol. 287, R161–R166.
Auguste, P., Hugues, M., Gravé, B., Gesquière, J.C., Maes, P., Tartar, A., Romey, G., Schweitz, H., Lazdunski, M., 1990. Leiurotoxin I (scyllatoxin), a peptide ligand for Ca^{2+}-activated K^+ channels. J. Biol. Chem. 265, 4753–4759.
Blatz, A., Magleby, K.L., 1986. Single apamin-blocked Ca-activated K^+ channels of small conductance in cultured rat skeletal muscle. Nature 323, 718–720.
Blatz, A., Magleby, K.L., 1987. Calcium-activated potassium channels. Trends. Neurosci. 10, 463–467.
Candia, S., Garcia, M.L., Latorre, R., 1992. Mode of action of iberiotoxin, a potent blocker of the large conductance Ca^{2+}-activated K^+ channel. Biophys. J. 63, 583–590.
Coupland, R.E., 1965. The Natural History of the Chromaffin Cell. Longmans, London.
Coupland, R.E., 1984. Ultrastructural features of the mammalian adrenal medulla. In: Motta, P.M. (Ed.), Ultrastructure of Endocrine Cells and Tissues. Nijhoff, Boston, MA, pp. 168–179.
Flink, M.T., Atchison, W.D., 2003. Iberiotoxin-induced block of Ca^{2+}-activated K^+ channels induces dihydropyridine sensitivity of ACh release from mammalian motor nerve terminals. J. Pharmacol. Exp. Ther. 305, 646–652.
Fukushima, Y., Nagayama, T., Hikichi, H., Mizukami, K., Yoshida, M., Suzuki-Kusaba, M., Hisa, H., Kimura, T., Satoh, S., 2002. Role of K^+ channels in the PACAP-induced catecholamine secretion from the rat adrenal gland. Eur. J. Pharmacol. 437, 69–72.
García, A.G., García-De-Diego, A.M., Gandía, L., Borges, R., García-Sancho, J., 2006. Calcium signaling and exocytosis in adrenal chromaffin cells. Physiol. Rev. 86, 1093–1131.
Garcia, M.L., Galvez, A., Garcia-Calvo, M., King, V.F., Vazquez, J., Kaczorowski, G.J., 1991. Use of toxins to study potassium channels. J. Bioenerg. Biomembr. 23, 615–646.
Kanus, H.G., McManus, O.B., Lee, S.H., Schmalhofer, W.A., Galcia-Calvo, M., Helms, L.M., Sanchez, M., Giangiacomo, K., Reuben, J.P., Smith, A.B., 1994. Tremorgenic indole alkaloids potently inhibit smooth muscle high-conductance calcium-activated potassium channels. Biochemistry 33, 5819–5828.
Meir, A., Ginsburg, S., Butkevich, A., Kachalsky, S.G., Kaiserman, I., Ahdut, R., Demirgoren, S., Rahamimoff, R., 1999. Ion channels in presynaptic nerve terminals and control of transmitter release. Physiol. Rev. 79, 1019–1088.
Montiel, C., López, M.G., Sánchez-García, P., Maroto, R., Zapater, P., García, A.G., 1995. Contribution of SK and BK channels in the control of catecholamine release by electrical stimulation of the cat adrenal gland. J. Physiol. 486, 427–437.

Nagayama, T., Fukushima, Y., Hikichi, H., Yoshida, M., Suzuki-Kusaba, M., Hisa, H., Kimura, T., Satoh, S., 2000a. Interaction of SK_{Ca} channels and L-type Ca^{2+} channels in catecholamine secretion in the rat adrenal gland. Am. J. Physiol. 279, R1731–R1736.

Nagayama, T., Fukushima, Y., Yoshida, M., Suzuki-Kusaba, M., Hisa, H., Kimura, T., Satoh, S., 2000b. Role of potassium channels in catecholamine secretion in the rat adrenal gland. Am. J. Physiol. 279, R448–R454.

Nagayama, T., Masada, K., Yoshida, M., Suzuki-Kusaba, M., Hisa, H., Kimura, T., Satoh, S., 1998. Role of K^+ channels in adrenal catecholamine secretion in anesthetized dogs. Am. J. Physiol. 274, R1125–R1130.

Ohta, T., Ito, S., Nakazato, Y., 1998. Ca^{2+}-dependent K^+ currents induced by muscarinic receptor activation in guinea pig adrenal chromaffin cells. J. Neurochem. 70, 1280–1288.

Prakriya, M., Lingle, C.J., 1999. BK channel activation by brief deporalizations requires Ca^{2+} influx through L- and Q-type Ca^{2+} channels in rat chromaffin cells. J. Neurophysiol. 81, 2267–2278.

Sun, X.P., Schlichter, L.C., Stanley, E.F., 1999. Single-channel properties of BK-type calcium-activated potassium channels at a cholinergic presynaptic nerve terminal. J. Physiol. 518, 639–651.

Uceda, G., Artalejo, A.R., López, M.G., Abad, F., Neher, E., García, A.G., 1992. Ca^{2+}-activated K^+ channels modulate muscarinic secretion in cat chromaffin cells. J. Physiol. 454, 213–230.

Wada, A., Urabe, M., Yuhi, T., Yamamoto, R., Yanagita, T., Niina, H., Kobayashi, H., 1995. Large- and small-conductance Ca^{2+}-activated K^+ channels: their role in the nicotinic receptor-mediated catecholamine secretion in bovine adrenal medulla. Naunyn Schmiedeberg's Arch. Pharmacol. 352, 545–549.

Winer, B.J., 1971. Statistical Principles in Experimental Design, 2nd ed. McGraw-Hill, New York.

Zhang, X.Y., Zhu, F.X., Robinson, N.E., 1998. Role of cAMP and neuronal K^+ channels on α_2-AR-induced inhibition of ACh release in equine trachea. Am. J. Physiol. 274, L827–L832.

An international compendium of mutations in the *SCN5A*-encoded cardiac sodium channel in patients referred for Brugada syndrome genetic testing

Jamie D. Kapplinger, BA,* David J. Tester, BS,* Marielle Alders, PhD,[†] Begoña Benito, MD,[‡]
Myriam Berthet, BA,[§ǁ] Josep Brugada, MD, PhD,[¶] Pedro Brugada, MD, PhD,[#]
Véronique Fressart, MD,[§ǁ**] Alejandra Guerchicoff, PhD,[††] Carole Harris-Kerr, PhD,[‡‡]
Shiro Kamakura, MD, PhD,[§§] Florence Kyndt, PhD,[ǁǁ¶¶##] Tamara T. Koopmann, PhD,[***]
Yoshihiro Miyamoto, MD,[†††] Ryan Pfeiffer, BS,[††] Guido D. Pollevick, PhD,[‡‡]
Vincent Probst, MD, PhD,[ǁǁ##] Sven Zumhagen, MD,[‡‡‡] Matteo Vatta, PhD,[§§§] Jeffrey A. Towbin, MD,[ǁǁǁǁ]
Wataru Shimizu, MD, PhD,[§§] Eric Schulze-Bahr, MD,[‡‡‡] Charles Antzelevitch, PhD,[††]
Benjamin A. Salisbury, PhD,[‡‡] Pascale Guicheney, PhD,[§ǁ**] Arthur A. M. Wilde, MD, PhD,[***]
Ramon Brugada, MD, PhD,[¶¶¶¶] Jean-Jacques Schott, PhD,[ǁǁ¶¶###] Michael J. Ackerman, MD, PhD*

From the *Departments of Medicine, Pediatrics, and Molecular Pharmacology and Experimental Therapeutics/Divisions of Cardiovascular Diseases and Pediatric Cardiology, Windland Smith Rice Sudden Death Genomics Laboratory, Mayo Clinic, Rochester, Minnesota, †Department of Clinical Genetics, Academic Medical Centre, Amsterdam, the Netherlands, ‡Departamento de Biotecnología, Universidad Politécnica de Madrid, Madrid, Spain, §Inserm, U956, Groupe Hospitalier Pitié-Salpêtrière, Paris, France, ǁUPMC Univ Paris 06, UMR-S956, IFR14, Paris, France, ¶Hospital Clínic, University of Barcelona, Barcelona, Spain, #Heart Rhythm Management Centre, Cardiovascular Institute, UZ Brussel, VUB Brussels, Brussels, Belgium, **AP-HP, Groupe Hospitalier Pitié-Salpêtrière, Service de Biochimie, Unité de Cardiogénétique et Myogénétique, Paris, France, ††Masonic Medical Research Laboratory, Utica, New York, ‡‡PGxHealth, LLC, a division of Clinical Data, Inc., New Haven, Connecticut, §§Division of Cardiology, Department of Internal Medicine, National Cardiovascular Center, Suita, Japan, ǁǁInstitut National de la Sante et de la Recherche Medicale, UMR 915, F-44000 Nantes, France, ¶¶CNRS ERL3147, F-44000 Nantes, France, ##Service de Cardiologie, L'Institut du Thorax Centre Hospitalier Universitaire de Nantes, F-44000 Nantes, France, ***Heart Failure Research Centre, Department of Cardiology, Academic Medical Centre, Amsterdam, the Netherlands, †††Laboratory of Molecular Genetics, National Cardiovascular Center, Suita, Japan, ‡‡‡Genetics of Heart Diseases, Hospital of the University of Münster, Germany, §§§Department of Pediatrics (Cardiology) and Department of Molecular Physiology and Biophysics, Baylor College of Medicine, Houston, Texas, ǁǁǁǁThe Heart Institute, Cincinnati Children's Hospital Medical Center, Cincinnati, Ohio, ¶¶¶¶Cardiovascular Genetics Center, School of Medicine, University of Girona, Spain, and ###Faculté de Médecine, L'Institut du Thorax, Université de Nantes, F-44000 Nantes, France.

BACKGROUND Brugada syndrome (BrS) is a common heritable channelopathy. Mutations in the *SCN5A*-encoded sodium channel (BrS1) culminate in the most common genotype.

OBJECTIVE This study sought to perform a retrospective analysis of BrS databases from 9 centers that have each genotyped >100 unrelated cases of suspected BrS.

METHODS Mutational analysis of all 27 translated exons in *SCN5A* was performed. Mutation frequency, type, and localization were compared among cases and 1,300 ostensibly healthy volunteers including 649 white subjects and 651 nonwhite subjects (blacks, Asians, Hispanics, and others) that were genotyped previously.

RESULTS A total of 2,111 unrelated patients (78% male, mean age 39 ± 15 years) were referred for BrS genetic testing. Rare mutations/variants were more common among BrS cases than control subjects (438/2,111, 21% vs. 11/649, 1.7% white subjects and 31/651, 4.8% nonwhite subjects, respectively, $P < 10^{-53}$). The yield of BrS1 genetic testing ranged from 11% to 28% ($P = .0017$). Overall, 293 distinct mutations were identified in *SCN5A*: 193 missense, 32 nonsense, 38 frameshift, 21 splice-site, and 9 in-frame deletions/insertions. The 4 most frequent BrS1-associated mutations were E1784K (14×),

F861WfsX90 (11×), D356N (8×), and G1408R (7×). Most mutations localized to the transmembrane-spanning regions.

CONCLUSION This international consortium of BrS genetic testing centers has added 200 new BrS1-associated mutations to the public domain. Overall, 21% of BrS probands have mutations in *SCN5A* compared to the 2% to 5% background rate of rare variants reported in healthy control subjects. Additional studies drawing on the data presented here may help further distinguish pathogenic mutations from similarly rare but otherwise innocuous ones found in cases.

KEYWORDS Brugada syndrome; Genetic testing; Ion channels; Sodium channel; Sudden death

ABBREVIATIONS BrS = Brugada syndrome; **BrS1** = Brugada syndrome type 1; **ChIPs** = sodium channel interacting proteins; **ECG** = electrocardiographic; **IDL** = interdomain linker; I_{Na} = available sodium current; **LQT3** = long-QT syndrome type 3; **LQTS** = long-QT syndrome; **MAF** = minor allele frequency; **PCR** = polymerase chain reaction; **SCD** = sudden cardiac death

(Heart Rhythm 2010;7:33–46) © 2010 Published by Elsevier Inc. on behalf of Heart Rhythm Society.

Introduction

Brugada syndrome (BrS) is a rare heritable arrhythmia syndrome characterized by an electrocardiographic (ECG) pattern consisting of coved-type ST-segment elevation in the right precordial leads V_1 through V_3 (often referred to as a type-1 Brugada ECG pattern) and an increased risk for sudden cardiac death (SCD).[1,2] The penetrance and expressivity of this autosomal-dominant disorder is highly variable, ranging from a lifelong asymptomatic course to SCD during the first year of life. The syndrome is thought to account for up to 4% of all SCDs and 20% of unexplained sudden death in the setting of a structurally normal heart;[3] however, some patients display a more benign course. BrS is generally considered a disorder involving young male adults, with arrhythmogenic manifestation first occurring at an average age of 40 years, with sudden death typically occurring during sleep.[4] However, BrS has also been demonstrated in children and infants as young as 2 days old and may serve as a pathogenic basis for some cases of sudden infant death syndrome.[3]

Since the disorder's sentinel clinical and ECG description in 1992 by Drs. Pedro and Josep Brugada,[5] *SCN5A*-encoded cardiac sodium channel loss-of-function mutations have been shown to confer the pathogenic basis for an estimated 15% to 30% of BrS, currently representing the most common BrS genotype and classified as Brugada syndrome type 1 (BrS1).[6–8] Loss-of-function mutations in *SCN5A* reduce the overall available sodium current (I_{Na}) through either impaired intracellular trafficking of the ion channel to the plasma membrane, thereby reducing membrane surface channel expression, or through altered gating properties of the channel. Gain-of-function *SCN5A* mutations cause a clinically and mechanistically distinct arrhythmia syndrome, long-QT syndrome type 3 (LQT3). Interestingly, some identical *SCN5A* mutations may provide either a loss-of-function BrS1-phenotype or a gain-of-function LQT3-phenotype, depending on the individual host.

In fact, LQT3/BrS/conduction-disorder *SCN5A* overlap syndromes do exist within single large families.[9,10]

After a decade of genetic testing by research laboratories worldwide, BrS genetic testing has made the transition from discovery to translation to clinical implementation with the availability of clinical BrS1 genetic testing (since 2004 in North America and even earlier in Europe), which provides comprehensive open-reading frame and canonical splice site mutational analysis of *SCN5A*. However, it must be recognized that nearly 2% of healthy Caucasians and 5% of healthy nonwhite subjects also host rare missense *SCN5A* variants, leading to a potential conundrum in the interpretation of the genetic test results.[11] Distinguishing pathogenic mutations from rare harmless genetic variants is of critical importance in the interpretation of genetic testing and the management of genotype-positive BrS patients.

Presently, there are over 100 BrS1-associated mutations publicly available (http://www.fsm.it/cardmoc). We sought to assemble an international compendium of putative BrS1-associated mutations through a retrospective analysis of BrS genomic databases from 9 reference centers throughout the world (5 Europe, 3 United States, 1 Japan) that have each genotyped >100 unrelated cases of clinically suspected BrS. Such a compendium may illuminate further key structure–function properties and provide a foundational building block for the development of algorithms to assist in distinguishing pathogenic mutations from similarly rare but otherwise innocuous ones.

Methods
Study population
A retrospective analysis of BrS databases from 9 centers throughout the world that have each genotyped >100 unrelated cases of clinically suspected BrS was performed. In total, 2,111 unrelated patients (78% male, mean age 39 ±

Table 1   Demographics and mutation yield for 9 Brugada syndrome genetic testing centers

	1	2	3	4	5	6	7	8	9
Total	451	365	311	237	195	158	153	130	111
Positive	92	88	69	50	44	26	43	14	12
Age (yrs)	47 ± 14	40 ± 11	45 ± 18	43 ± 14	35 ± 18	36 ± 21	45 ± 15	48 ± 10	37 ± 21
Range (yrs)	3 to 70	0 to 77	0 to 82	8 to 80	0 to 76	0 to 69	5 to 65	28 to 64	7 to 78
Yield (%)	20.4	24.1	22.2	21.1	22.6	16.5	28.1	10.8	10.8
Male	357	277	239	193	140	117	106	124	72
Positive	68	67	55	40	31	17	30	13	7
Yield (%)	21.6	24.2	22.2	20.7	23.4	14.5	28.3	10.5	9.7
Female	94	88	72	44	55	41	47	6	39
Positive	23	19	14	10	13	9	13	1	5
Yield (%)	25.5	21.6	19.4	22.7	23.6	22.0	27.7	16.7	12.8

Center: 1 = Nantes, 2 = Brugada, 3 = AMC, 4 = Paris, 5 = PGxHealth, 6 = MMRL, 7 = UKM, 8 = NCVC, 9 = BCM.

15 years) were referred for *SCN5A* genetic testing (Table 1). For the purpose of this compendium of identified mutations, only minimal demographic information for each center's cohort, such as the average age and range of age at diagnosis and the number of male and female subjects was provided. The specific age and gender were collected for mutation-positive patients. A sample was accepted for genetic testing if the referring physician had made a clinical diagnosis of either possible or definite BrS. An ECG was not always available for each patient. Although DNA samples were accepted for analysis based on a referral diagnosis of BrS, several of the international centers did collect and examine 12-lead ECGs to confirm the presence of an ECG pattern consistent with BrS.

Mutational analysis

Patient genomic DNA was analyzed for mutations in all 27 translated exons, including splice sites and adjacent regions, of the *SCN5A*-encoded cardiac sodium channel Na$_v$1.5 using a combination of polymerase chain reaction (PCR), either denaturing high-performance liquid chromatography or single-stranded conformation polymorphism and DNA sequencing.[12] In addition, frequency, location, and mutation type of *SCN5A* genetic variation found among 1,300 ostensibly healthy volunteers,[11,13] including 649 white subjects and 651 nonwhite subjects (black, Asian, and Hispanic), was analyzed and compared with the possible BrS1-associated mutations. To be reported in this compendium as a possible BrS1-associated mutation, the case mutation must have been absent among all 1,300 control subjects who underwent comprehensive mutation scanning. Further, each reference center examined a local set of control samples from usually 200 to 400 additional unrelated, healthy individuals to determine the presence or absence of each possible case mutation observed in patients from their respective geographical region.

Mutation nomenclature

All possible BrS1-associated mutations were denoted using the accepted Human Genome Variation Society's guidelines for nomenclature.[14] The nucleotide and amino acid designations were based on the *SCN5A* transcript NM_198056.2. For ex-

ample, the missense mutation E1784K would indicate the wild-type amino acid (E = glutamic acid) at position 1784 is replaced by lysine (K). Frameshift mutations resulting from nucleotide insertions or deletions were annotated using the F861WfsX90 format, which indicates that the wild-type phenylalanine (F) at position 861 is altered to a tryptophan (W) followed by 89 miscoded amino acids prior to a termination codon (X) 90 residues from the beginning of the altered reading frame.

A substitution of either the first or the last 2 nucleotides of a particular exon has the capacity to alter proper mRNA splicing, regardless of whether the nucleotide substitution codes for a different amino acid (missense mutation) produces a stop codon (nonsense mutation) or does not alter the open reading frame at all (i.e., a synonymous or silent single-nucleotide substitution).[15–17] As such, mutations involving this exonic portion of the splice site were considered as possible splicing mutations in this study and annotated as either missense/splice-site, nonsense/splice-site, or silent/splice-site mutations to distinguish them from intronic mutations predicted to disrupt splicing.

Topological placement of the mutations was assigned using a combination of Swissprot (http://ca.expasy.org/uniprot/) and recent studies of the linear topologies for the sodium channel pore-forming alpha subunit.[18–20] The Swissprot database provides generally accepted residue ranges corresponding with each ion-channel region and specialized subregions. For Nav1.5, mutations were localized to either the N-terminus (amino acids 1 to 126), interdomain linker (IDL I-II, aa 416-711, IDL II-III, aa 940-1200, and IDL III-IV, aa 1471-1523), transmembrane/linker (Domain I, aa 127-415, Domain II, aa 712-939, Domain III, aa 1201-1470, Domain IV, aa 1524-1772), or C-terminus (aa 1773-2016). The transmembrane-spanning region was further subdivided into S1 through S4 (DI S1-S4/S5, aa 127-252, DII S1-S4/S5, aa 712-841, DIII S1-S4/S5, aa 1201-1336, and DIV S1-S4/S5, aa 1524-1659) and S5 through S6, the pore region and selectivity filter of the channel (DI S5-S6, aa 253-415, DII S5-S6, aa 842-939, DIII S5-S6, aa 1337-1470, DIV S5-S6, aa 1660-1772).

Defining terminology: variant versus mutation

For the purposes of this compendium, a variant will be defined as any change to the wild-type sequence, whether it is in case or control subjects. Mutations will be identified as rare, case-only (absent in the 1,300+ healthy volunteers) variants that are possibly pathogenic. Variants identified with a minor allele frequency (MAF) >0.5% among the 1,300 healthy control subjects will be termed common polymorphisms. If the MAF is <0.5%, these variants will be termed uncommon/rare polymorphisms.

Defining a variant as a possible BrS1-causative mutation

To be considered as a possible BrS1-causing mutation, the variant must disrupt either the open reading frame (i.e., missense, nonsense, insertion/deletion, or frameshift mutations) or the splice site (polypyrimidine tract, splice acceptor, or splice donor recognition sequences). In addition to the exonic splice sites described above, the acceptor splice site was defined as the 3 intronic nucleotides preceding an exon (designated as IVS-1, -2, or -3) and the donor splice site as the first 5 intronic nucleotides after an exon (designated as IVS+1, +2, +3, +4, or +5).[17] Additionally, single-nucleotide substitutions (namely, a purine [A or G] for a pyrimidine [C or T]) within the polypyrimidine tract immediately preceding the acceptor splice-site may be causative.[17] As such, some pyrimidine-to-purine substitutions in this region of the intron have been included as potentially pathogenic. For example, an IVS-5 cytosine (C) that falls within the polypyrimidine tract and is substituted by an adenine (A) that would predictably disrupt the polypyrimidine tract and consequently result in aberrant splicing would be included as a possible pathogenic mutation. Hence, single-nucleotide substitutions that obviously did not change the open reading frame (i.e., synonymous single-nucleotide polymorphisms) or those outside of the splice site recognition sequence were not included in either case or control subjects for this study.

Additionally, to be considered as a possible BrS1-causing mutation, the nonsynonymous variant must have been absent in all published databases listing the SCN5A channel common polymorphisms and previously published reports or compendia of rare control variants, e.g., those found in over 2,600 reference alleles (Table 2) derived from over 1,300 ostensibly healthy adult volunteers.[11,13] As such, the sole or concomitant presence of a common polymorphism such as H558R-SCN5A or a rarer polymorphism such as A572D-SCN5A would not by definition warrant the annotation of possible BrS1-associated mutation and would not be counted toward the assignment of compound or multiple mutation status to an individual in this compendium. This does not imply that common and rare polymorphisms may not possibly modulate the BrS1 phenotype.

Results

Overall, 2,111 unrelated patients (78% male, average age at testing 39 ± 15 years) were referred for BrS genetic testing across 9 testing centers (Table 1). As expected, rare SCN5A missense mutations were far more common among BrS cases (438/2,111, 21%) than similarly rare genetic variants were among control subjects (43/1,300 [11/649, 1.7% white subjects and 31/651, 4.8% nonwhite subjects], $P < 10^{-55}$). The yield differed significantly across centers ($P = .0017$; $chi^2 = 24.7$, degrees of freedom (df) = 8), ranging from 11% (centers 8 [14/130] and 9 [12/111]) to 28% (center 7 [43/153], $P = .0017$ for the 9 centers) (Table 1, Figure 1). There was no significant difference in yield between male (324/1,520, 21.3%) and female (112/439, 25.5%, $P = .07$) subjects. Of the 438 SCN5A mutation-positive cases, 13 (3%) harbored multiple mutations (Table 3). All 13 were male and trended toward younger age at diagnosis (29.7 ± 16.2 years) than male subjects with a single mutation (39.2 ± 14.4 years, $P = .07$).

Overall, 293 distinct, possible BrS1-associated mutations (200, 68% novel to this cohort), absent in 2,600 reference alleles, were identified in the 438 genotype-positive cases, 225 (77%) of which were identified only once (Table 4, Figure 2). Only 68 mutations were found in multiple unrelated patients. The 4 most frequent BrS1-associated mutations were E1784K (14 patients), F861WfsX90 (11 patients), D356N (8 patients), and G1408R (7 patients) (Table 4, Figure 2). Two-thirds of the unique mutations were missense mutations (193), whereas the remaining third (100) involved radical mutations (38 frameshift, 32 nonsense, 21 splice-site, and 9 in-frame insertions or deletions) (Table 4, Figure 3).

Of the 293 unique mutations, 208 (71%) localized to one of the 4 transmembrane-spanning regions (DI, DII, DIII, or DIV), 54 (18%) localized to an IDL (31 in IDL I-II, 17 in IDL II-III, and 6 in IDL III-IV), 17 (6%) localized to the C-terminus, and 14 (5%) localized to the N-terminus (Table 4, Figure 4). The majority of patients with a single SCN5A mutation (313/425, 74%) hosted a mutation that localized to the transmembrane region of the channel, with 31% (133/425) having a mutation that localized to either DI S1-S4, DII S1-S4, DIII S1-S4, or DIV S1-S4 and 42% (180/425) having a mutation that localized to the S5, P-loop, and S6 regions containing the pore and selectivity filter of the sodium channel (DI S5-S6, DII S5-S6, DIII S5-S6, or DIV S5-S6) (Table 4, Figure 4). In fact, compared with the topological location for the rare control variants, there was a strong predilection for a patient's possible BrS1-associated mutation to localize to the channel's transmembrane (S1-S4 6.3% vs. 0.2%, $P < 10^{-24}$) and pore-forming segments (S5-S6 8.5% vs. 0.5%, $P < 10^{-30}$) (Figure 5). Twenty-eight patients (1.3%) had their possible BrS1-associated missense mutation localizing to the DI-DII or DII-DIII linker domains, where the vast majority of the rare missense SCN5A variants, which were discovered among the ostensibly healthy control subjects, reside. The yield for the linker regions was 3% for cases compared with 1.7% for healthy subjects ($P = NS$) (Figure 5).

Interestingly, 10 (3.4%) of the mutations, identified in 29 patients of this BrS compendium, have been identified previously in cases of long-QT syndrome (LQTS): G615E, L619F, E1225K, P1332L, L1501V, R1623Q, I1660V, V1667I, T1779M, including the most common BrS1-associated muta-

Table 2   Control variants found in 2,600 reference alleles

Exon	Nucleotide change	Variant	Mutation type	Location	Number	Ethnicity	Status
2	52 C>T	R18W	Missense	N-terminal	1	O	Rare control
2	100 C>T	R34C	Missense	N-terminal	44	B>H=O>W>A	Polymorphism
2	101 G>A	R34H	Missense	N-terminal	1	B	Rare control
6	647 C>T	S216L	Missense	DI-S3/S4	4	W	Polymorphism
7	856 G>T	A286S	Missense	DI-S5/S6	1	B	Rare control
7	872 A>G	N291S	Missense	DI-S5/S6	1	O	Rare control
7	895 T>A	L299M	Missense	DI-S5/S6	1	B	Rare control
9	1126 C>T	R376C	Missense	DI-S5/S6	1	W	Rare control
11	1340 C>G	A447G	Missense	DI/DII	1	B	Rare control
11	1345 A>G	T449A	Missense	DI/DII	1	O	Rare control
11	1381 T>G	L461V	Missense	DI/DII	2	B	Polymorphism
11	1425 A>C	R475S	Missense	DI/DII	1	B	Rare control
11	1441 C>T	R481W	Missense	DI/DII	6	B>H=O	Polymorphism
12	1571 C>A	S524Y	Missense	DI/DII	18	B>W=H	Polymorphism
12	1673 A>G	H558R	Missense	DI/DII	408	W>B>H>O>A	Polymorphism
12	1703 G>A	R568H	Missense	DI/DII	1	W	Rare control
12	1735 G>A	G579R	Missense	DI/DII	1	W	Rare control
12	1776 C>A	N592K	Missense	DI/DII	1	W	Rare control
12	1787 A>G	D596G	Missense	DI/DII	1	B	Rare control
12	1802 T>C	V601A	Missense	DI/DII	1	W	Rare control
12	1852 C>T	L618F	Missense	DI/DII	1	O	Rare control
13	1913 G>A	G638D	Missense	DI/DII	1	A	Rare control
13	1967 C>T	P656L	Missense	DI/DII	1	B	Rare control
13	2014 G>A	A672T	Missense	DI/DII	1	A	Rare control
14	2066 G>A	R689H	Missense	DI/DII	1	H	Rare control
14	2074 C>A	Q692K	Missense	DI/DII	3	W	Polymorphism
14	2114 C>T	S705F	Missense	DI/DII	1	A	Rare control
16	2770 G>A	V924I	Missense	DII-S6	2	B=O	Polymorphism
17	2924 C>T	R975W	Missense	DII/DIII	1	W	Rare control
17	2957 G>A	R986Q	Missense	DII/DIII	1	B	Rare control
17	3047 C>T	T1016M	Missense	DII/DIII	1	A	Rare control
17	3118 G>A	G1040R	Missense	DII/DIII	1	B	Rare control
18	3245 T>C	V1082A	Missense	DII/DIII	1	B	Rare control
18	3269 C>T	P1090L	Missense	DII/DIII	5	A>W	Polymorphism
18	3292 G>T	V1098L	Missense	DII/DIII	1	A	Rare control
18	3308 C>A	S1103Y	Missense	DII/DIII	31	B>O>H	Polymorphism
18	3319 G>A	E1107K	Missense	DII/DIII	1	A	Rare control
18	3346 C>T	R1116W	Missense	DII/DIII	2	A	Polymorphism
20	3578 G>A	R1193Q	Missense	DII/DIII	12	A>W	Polymorphism
21	3751 G>A	V1251M	Missense	DIII-S2	1	B	Rare control
22	3878 T>C	F1293S	Missense	DIII-S3/S4	2	W	Polymorphism
22	3922 C>T	L1308F	Missense	DIII-S4	3	O>B	Polymorphism
Intron 24	4299 +2 T>A	1433sp	Splice site	DIII-S5/S6	1	W	Rare control
26	4534 C>T	R1512W	Missense	DIII/DIV	1	H	Rare control
28	5360 G>A	S1787N	Missense	C-terminal	3	W	Polymorphism
28	5507 T>C	I1836T	Missense	C-terminal	1	B	Rare control
28	5701 G>A	E1901K	Missense	C-terminal	1	W	Rare control
28	5755 C>T	R1919C	Missense	C-terminal	1	B	Rare control
28	5851 G>T	V1951L	Missense	C-terminal	16	H>A>B=O	Polymorphism
28	5873 G>A	R1958Q	Missense	C-terminal	1	B	Rare control
28	5885 C>T	P1962L	Missense	C-terminal	1	B	Rare control
28	5904 C>G	I1968M	Missense	C-terminal	1	B	Rare control
28	5972 G>A	R1991Q	Missense	C-terminal	1	B	Rare control
28	6010 T>C	F2004L	Missense	C-terminal	7	W>H	Polymorphism
28	6016 C>G	P2006A	Missense	C-terminal	3	W>B	Polymorphism

The > and = symbols represent the relative prevalence of the variant of interest in each corresponding ethnicity.
A = Asian; B = black; H = Hispanic; O = other; and W = white.

tion, E1784K, observed in this BrS compendium. Five of the 10 have been functionally characterized previously, with L619F,[21] P1332L,[22] R1623Q,[23] and E1784K[24] producing channel abnormalities consistent with an LQT3 phenotype and G615E[25] producing a wild-type–like SCN5A channel.[10]

Discussion
Since the first report by Chen et al[26] in 1998, a little over 100 unique *SCN5A* mutations have been implicated as possibly causative for BrS1. Previous small cohort studies have indicated that the prevalence of *SCN5A* mutations in BrS is
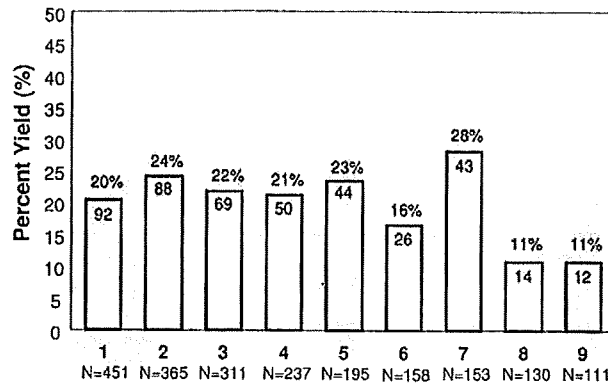
Figure 1 Mutation detection yield by genetic testing center. Depicted here is a comparison of Brugada syndrome genetic testing for each of the 9 centers ordered according to the total number (N = X) of unrelated patients tested. The number within each column represents the number of genotype positive patients for the respective center. For example, Center 1 analyzed 451 unrelated cases and identified a putative pathogenic mutation in 92 (20%). Center: 1 = Nantes, 2 = Brugada, 3 = AMC, 4 = Paris, 5 = PGxHealth, 6 = MMRL, 7 = UKM, 8 = NCVC, 9 = BCM.

roughly 15% to 20%, and possibly as high as 40% in cases of familial BrS. In 2000, Priori et al[6] reported a 15% yield with respect to SCN5A mutations among 52 unrelated patients. In 2002, these investigators extended their analysis to 130 probands (20% with a family history of sudden unexplained death) and identified an SCN5A mutation in 22%.[7] Schulze-Bahr et al[8] reported a 14% yield among 44 unrelated BrS patients, who are included in the current compendium.

Here, through this international multicenter study, we provide an expanded compendium of 293 unique (200 novel) BrS1-associated SCN5A mutations derived from over 2,100 unrelated patients referred for BrS genetic testing. The overall yield was 21% and ranged from 11% to 28% among the 9 centers. The differences in yield between the centers may be due to technical differences in mutational analysis methods used among laboratories, but it more likely reflects phenotypic differences among cohorts. For example, the cohorts with the lowest yield may have a preponderance of sporadic cases compared with familial cases. In 2003, Schulze-Bahr et al[8] reported that although none of their 27 sporadic BrS cases hosted an SCN5A mutation, 38% of their index cases with clearly familial BrS were positive. The number of sporadic versus familial BrS patients for each center's cohort is currently unknown. Alternatively, some of the lower yield centers may have accepted a greater proportion of weaker clinical cases for BrS genetic testing because no particular litmus test was demanded before acceptance of a sample.

Eight of the 9 centers represent research-based genetic testing laboratories, where most often the cohorts for such laboratories are composed of phenotypically robust cases of BrS. However, 1 center (center 5 in Table 1) represents a clinical laboratory offering the commercially available, fee-based genetic test for both BrS1 and LQTS. In this setting, the level of clinical suspicion and the usage of the genetic test by the referring physician are unknown for each patient sample submitted. Among their first 195 BrS referral cases submitted for

clinical genetic testing, 22.6% were identified with a possible pathogenic SCN5A mutation, which is in line with the higher point estimate of a 20% prevalence of SCN5A mutations among clinically strong cases of BrS patients,[7] and consistent with the noncommercial centers in this compendium. In contrast, this laboratory has reported a yield of 36% for the first 2,500 consecutive unrelated LQTS referral cases tested compared with a yield of 75% among clinically strong cases of LQTS.[27] These observations suggest that in clinical practice, prescribing cardiologists are submitting higher-probability BrS cases for BrS1 genetic testing compared with LQTS.

In this compendium, 3% of the genotype-positive patients hosted multiple putative pathogenic SCN5A mutations, absent in control subjects. Akin to genotype–phenotype observations in LQTS,[28] patients hosting multiple SCN5A mutations were younger at diagnosis (29.7 ± 16 years) than those having a single mutation. Nearly half of the 13 cases (all male) with multiple mutations were younger than 25 years of age, with the youngest presenting at 2 years of age. Whether carriers of multiple mutations had a more severely expressed phenotype, such as having more multiple syncopal events, aborted cardiac arrest, or stronger family history of SCD, than single-mutation carriers is unknown.

Mutations in this compendium overwhelmingly represent "private" mutations, meaning they were seen only once. Nearly 80% of the 293 unique mutations were identified in a single unrelated case. Fewer than 20 mutations were seen in more than 3 unrelated BrS patients. However, nearly 10% of the 438 unrelated SCN5A mutation-positive patients hosted 1 of 4 mutations: E1784K (14 patients), F861WfsX90 (11 patients), D356N (8 patients), and G1408R (7 patients). In this compendium, more than one-third of the genotype-positive patients had radical or non-missense mutations (i.e., frameshift, nonsense, and splicing errors) that represent extremely high-probability case mutations (only 1 such variant was found in 1 of the 1,300 healthy volunteers) and would predictably cause a

Table 3 Brugada syndrome patients with multiple SCN5A mutations

Gender	Age at diagnosis (yrs)	Mutation 1	Location	Mutation 2	Location
M	35	N109K	N-terminal	V240M	DI-S4/S5
M	16	A185V	DI-S2/S3	A226V	DI-S4
M	44	611+1 G>A	DI-S3	V300I	DI-S5/S6
M	26	T220I	DI-S4	E439K	DI-DII
M	21	934+4 C>T	DI-S5/S6	G1642E	DIV-S4
M	51	P336L	DI-S5/S6	I1660V	DIV-S5
M	40	L619F	DI-DII	Q1383X	DII-S5/S6
M	49	T632M	DI-DII	M764R	DII-S2
M	2	Q646RfsX5	DI-DII	D1243N	DIII-S2
M	24	A647D	DI-DII	P1332L	DIII-S4/S5
M	7	G752R	DII-S2	K1872N	C-terminal
M	41	E1053K	DII-DIII	R1583C	DIV-S2/S3
M	23	R1232W	DIII-S1/S2	T1620M	DIV-S3/S4

M = male.

Table 4   Compendium of Brugada syndrome-associated *SCN5A* mutations

Region	Nucleotide change	Coding effect	Mutation type	Location	No. of unrelated individuals	Testing center
Exon 2	3 G>A	M1I*	Missense	N-terminal	1	1
Exon 2	53 G>A	R18Q*	Missense	N-terminal	1	3
Exon 2	191_193delTGC	L64del*	In-frame del	N-terminal	1	5
Exon 2	210 T>G	N70K*	Missense	N-terminal	1	5
Exon 2	217 C>T	Q73X*	Nonsense	N-terminal	1	2
Exon 2	250 G>A	D84N*	Missense	N-terminal	2	1
Exon 3	278 T>C	F93S*	Missense	N-terminal	1	1
Exon 3	281 T>G	I94S*	Missense	N-terminal	1	7
Exon 3	310 C>T	R104W*	Missense	N-terminal	2	1, 2
Exon 3	311 G>A	R104Q	Missense	N-terminal	3	1, 7, 8
Exon 3	327 C>A	N109K*	Missense	N-terminal	1	3
Exon 3	361 C>T	R121W*	Missense	N-terminal	1	8
Exon 3	362 G>A	R121Q*	Missense	N-terminal	2	2, 6
Exon 3	376 A>G	K126E	Missense	N-terminal	1	9
Exon 3	381dupT	L128SfsX44*	Frame shift	DI-S1	1	7
Intron 3	393 −5 C>A*		Splice site	DI-S1	1	1
Exon 4	407 T>C	L136P	Missense	DI-S1	2	8
Exon 4	410_418dupTCATGTGCA	I137_C139dup*	In-frame ins	DI-S1	1	3
Exon 4	436 G>A	V146M*	Missense	DI-S1	1	7
Exon 4	468 G>A	W156X	Nonsense	DI-S1/S2	1	3
Exon 4	477 T>A	Y159X*	Nonsense	DI-S2	1	5
Exon 4	481 G>C	E161Q*	Missense	DI-S2	1	6
Exon 4	481 G>A	E161K	Missense	DI-S2	3	3, 4
Exon 5	486delC	Y162XfsX1*	Frame shift	DI-S2	1	5
Exon 5	525 G>C	K175N*	Missense	DI-S2	1	1
Exon 5	533 C>G	A178G*	Missense	DI-S2	1	9
Exon 5	535 C>T	R179X	Nonsense	DI-S2/S3	1	2
Exon 5	544 T>C	C182R*	Missense	DI-S2/S3	1	4
Exon 5	554 C>T	A185V*	Missense	DI-S2/S3	1	2
Exon 5	579 G>A	W193X*	Nonsense	DI-S3	1	4
Exon 5	611 C>T	A204V*	Missense	DI-S3	1	4
Intron 5	611 +1 G>A*		Splice site	DI-S3	1	5
Intron 5	611 +3_611+4dupAA		Splice site	DI-S3	1	9
Intron 5	612 −2 A>G*		Splice site	DI-S3	1	4
Exon 6	635 T>A	L212Q*	Missense	DI-S3/S4	1	5
Exon 6	656_657insATTCA	T220FfsX10*	Frame shift	DI-S4	1	2
Exon 6	659 C>T	T220I	Missense	DI-S4	2	2, 3
Exon 6	664 C>T	R222X	Nonsense	DI-S4	4	2, 4
Exon 6	665 G>A	R222Q	Missense	DI-S4	1	4
Exon 6	667 G>C	V223L*	Missense	DI-S4	2	2
Exon 6	673 C>T	R225W	Missense	DI-S4	3	1, 6
Exon 6	677 C>T	A226V	Missense	DI-S4	2	2
Exon 6	694 G>A	V232I	Missense	DI-S4	2	2, 6
Exon 7	718 G>A	V240M	Missense	DI-S4/S5	1	3
Exon 7	745 A>T	K249X*	Nonsense	DI-S4/S5	1	6
Exon 7	808 C>A	Q270K*	Missense	DI-S5	1	6
Exon 7	827 T>A	L276Q	Missense	DI-S5	1	8
Exon 7	832 C>G	H278D*	Missense	DI-S5/S6	1	4
Exon 7	844 C>T	R282C*	Missense	DI-S5/S6	1	2
Exon 7	898 G>A	V300I*	Missense	DI-S5/S6	1	5
Intron 7	934 +1 G>A*		Splice site	DI-S5/S6	1	3
Intron 7	934 +4 C>T*		Splice site	DI-S5/S6	1	5
Exon 8	944 T>C	L315P*	Missense	DI-S5/S6	1	6
Exon 8	959 C>A	T320N*	Missense	DI-S5/S6	1	5
Exon 8	974 T>G	L325R	Missense	DI-S5/S6	1	4
Intron 8	998 +1 G>A*		Splice site	DI-S5/S6	1	4
Exon 9	1007 C>T	P336L	Missense	DI-S5/S6	2	2, 6
Exon 9	1036 G>T	E346X	Nonsense	DI-S5/S6	1	1
Exon 9	1052 G>T	G351V	Missense	DI-S5/S6	1	9
Exon 9	1052 G>A	G351D*	Missense	DI-S5/S6	1	2
Exon 9	1066 G>A	D356N	Missense	DI-S5/S6	8	1, 2, 4, 6, 7
Exon 9	1099 C>T	R367C	Missense	DI-S5/S6	2	3
Exon 9	1100 G>T	R367L*	Missense	DI-S5/S6	1	1

Table 4 Continued

Region	Nucleotide change	Coding effect	Mutation type	Location	No. of unrelated individuals	Testing center
Exon 9	1100 G>A	R367H	Missense	DI-S5/S6	6	1, 2, 8, 9
Exon 9	1106 T>A	M369K	Missense	DI-S5/S6	1	1
Exon 9	1120 T>G	W374G*	Missense	DI-S5/S6	1	1
Exon 9	1127 G>A	R376H	Missense	DI-S5/S6	4	3, 4, 8
Exon 10	1156 G>A	G386R*	Missense	DI-S5/S6	1	1
Exon 10	1157 G>A	G386E*	Missense	DI-S5/S6	2	2
Exon 10	1186 G>C	V396L*	Missense	DI-S6	1	1
Exon 10	1187 T>C	V396A*	Missense	DI-S6	1	2
Exon 10	1255 C>T	Q419X*	Nonsense	DI/DII	1	7
Exon 10	1315 G>A	E439K*	Missense	DI/DII	1	3
Intron 10	1338 +2 T>A*		Splice site	DI/DII	1	6
Exon 11	1428_1431delCAAG	S476RfsX30*	Frame shift	DI/DII	1	3
Exon 11	1502 A>G	D501G	Missense	DI/DII	1	3
Exon 12	1537delC	R513VfsX8*	Frame shift	DI/DII	1	8
Exon 12	1562delA	K521SfsX102*	Frame shift	DI/DII	1	2
Exon 12	1577 G>A	R526H*	Missense	DI/DII	2	1, 5
Exon 12	1595 T>G	F532C	Missense	DI/DII	1	2
Exon 12	1603 C>T	R535X	Nonsense	DI/DII	4	1, 2, 4, 5
Exon 12	1629 T>A	F543L*	Missense	DI/DII	1	2
Exon 12	1654 G>A	G552R*	Missense	DI/DII	1	9
Exon 12	1717 C>T	Q573X*	Nonsense	DI/DII	1	2
Exon 12	1721delG	G574DfsX49*	Frame shift	DI/DII	1	2
Exon 12	1844 G>A	G615E	Missense	DI/DII	1	4
Exon 12	1855 C>T	L619F	Missense	DI/DII	1	1
Exon 12	1858 C>T	R620C*	Missense	DI/DII	1	1
Exon 12	1890 G>A	T630T*	Silent/splice site	DI/DII	3	1, 3
Intron 12	1890 +5 G>A*		Splice site	DI/DII	2	2, 5
Exon 13	1895 C>T	T632M	Missense	DI/DII	2	2, 4
Exon 13	1918 C>G	P640A*	Missense	DI/DII	1	3
Exon 13	1936delC	Q646RfsX5*	Frame shift	DI/DII	3	2, 5, 6
Exon 13	1940 C>A	A647D*	Missense	DI/DII	1	5
Exon 13	1943 C>T	P648L	Missense	DI/DII	1	7
Exon 13	1950_1953delAGAT	D651AfsX25*	Frame shift	DI/DII	1	4
Exon 13	1981 C>T	R661W*	Missense	DI/DII	1	5
Exon 13	1983_1993dupGGCCCTCAGCG	A665GfsX16*	Frame shift	DI/DII	1	1
Exon 14	2024_2025delAG	E675VfsX45*	Frame shift/splice	DI/DII	1	2
Exon 14	2047 T>G	C683G*	Missense	DI/DII	1	7
Exon 14	2092 G>T	E698X*	Nonsense	DI/DII	1	2
Exon 14	2102 C>T	P701L	Missense	DI/DII	1	4
Exon 14	2150 C>T	P717L*	Missense	DII-S1	1	6
Exon 14	2201dupT	M734IfsX11*	Frame shift	DII-S1	1	7
Exon 14	2204 C>T	A735V	Missense	DII-S1	4	2, 4, 8, 9
Exon 14	2236 G>A	E746K	Missense	DII-S1/S2	3	1, 2, 7
Exon 14	2254 G>A	G752R	Missense	DII-S2	5	1, 5
Exon 15	2273 G>A	G758E*	Missense	DII-S2	1	2
Exon 15	2274delG	I759FfsX6*	Frame shift	DII-S2	2	5
Exon 15	2291 T>G	M764R*	Missense	DII-S2	1	4
Exon 15	2314 G>A	D772N	Missense	DII-S2/S3	1	1
Exon 15	2317 C>T	P773S*	Missense	DII-S2/S3	1	6
Exon 15	2320delT	Y774TfsX28*	Frame shift	DII-S2/S3	2	3
Exon 15	2326_2328delTAC	Y776del*	In-frame del	DII-S2/S3	1	2
Exon 15	2365 G>A	V789I*	Missense	DII-S3	1	4
Exon 15	2423 G>C	R808P*	Missense	DII-S4	1	1
Exon 15	2435_2436+3delTGGTAinsCGCCT	L812P†*	Indel/splice site	DII-S4	1	5
Exon 16	2465 G>A	W822X	Nonsense	DII-S4	1	4
Exon 16	2516 T>C	L839P*	Missense	DII-S4/S5	1	1
Exon 16	2533delG	V845CfsX2*	Frame shift	DII-S5	1	6
Exon 16	2549_2550insTG	F851GfsX19*	Frame shift	DII-S5	1	2
Exon 16	2550_2551dupGT	F851CfsX19*	Frame shift	DII-S5	1	5
Exon 16	2553 C>A	F851L	Missense	DII-S5	1	2
Exon 16	2582_2583delTT	F861WfsX90	Frame shift	DII-S5	11	3, 7
Exon 16	2599 G>C	E867Q*	Missense	DII-S5/S6	1	2
Exon 16	2602delC	L868X	Frame shift	DII-S5/S6	2	6, 7

Table 4   Continued

Region	Nucleotide change	Coding effect	Mutation type	Location	No. of unrelated individuals	Testing center
Exon 16	2632 C>T	R878C	Missense	DII-S5/S6	1	2
Exon 16	2633 G>A	R878H*	Missense	DII-S5/S6	5	1, 2, 4, 5, 7
Exon 16	2657 A>C	H886P*	Missense	DII-S5/S6	1	2
Exon 16	2677 C>T	R893C*	Missense	DII-S5/S6	2	4
Exon 16	2678 G>A	R893H*	Missense	DII-S5/S6	3	1, 3, 4
Exon 16	2701 G>A	E901K*	Missense	DII-S5/S6	3	1, 4
Exon 16	2729 C>T	S910L	Missense	DII-S5/S6	1	1
Exon 16	2743 T>C	C915R*	Missense	DII-S6	1	3
Exon 16	2750 T>G	L917R*	Missense	DII-S6	1	2
Exon 16	2780 A>G	N927S	Missense	DII-S6	3	3, 7
Exon 16	2783 T>C	L928P*	Missense	DII-S6	1	1
Exon 17	2804 T>C	L935P*	Missense	DII-S6	1	5
Exon 17	2850delT	D951MfsX6*	Frame shift	DII/DIII	1	4
Exon 17	2893 C>T	R965C	Missense	DII/DIII	3	2, 4, 5
Exon 17	2894 G>A	R965H	Missense	DII/DIII	1	3
Exon 17	2914_2923delTTTGTCAAGC	F972GfsX170*	Frame shift	DII/DIII	1	6
Exon 17	2989 G>A	A997T*	Missense	DII/DIII	1	5
Exon 17	3005_3012delCCAGCTGC	P1002HfsX25*	Frame shift	DII/DIII	1	7
Exon 17	3140_3141dupTG	P1048CfsX98*	Frame shift	DII/DIII	1	3
Exon 17	3157 G>A	E1053K	Missense	DII/DIII	3	1
Exon 17	3164 A>G	D1055G*	Missense	DII/DIII	1	1
Exon 17	3171_3172delTGinsA	D1057EfsX88*	Insertion/deletion	DII/DIII	1	7
Intron 17	3228 +2delT*		Splice site	DII/DIII	1	3
Exon 18	3236 C>A	S1079Y*	Missense	DII/DIII	1	1
Exon 18	3338 C>T	A1113V*	Missense	DII/DIII	1	5
Exon 18	3345 G>A	W1115X*	Nonsense	DII/DIII	1	6
Exon 19	3419 G>C	S1140T*	Missense	DII/DIII	1	5
Exon 20	3553_3554delCA	Q1185GfsX55*	Frame shift	DII/DIII	1	3
Exon 20	3576 G>A	W1192X*	Nonsense	DII/DIII	1	6
Exon 20	3622 G>T	E1208X	Nonsense	DIII-S1	1	1
Exon 20	3634_3636delATC	I1212del*	In-frame del	DIII-S1	1	2
Exon 20	3656 G>A	S1219N	Missense	DIII-S1	1	1
Exon 20	3666delG	A1223PfsX7*	Frame shift/splice	DIII-S1	1	1
Exon 21	3673 G>A	E1225K	Missense	DIII-S1/S2	4	1, 5, 6, 7
Exon 21	3682 T>C	Y1228H	Missense	DIII-S1/S2	1	1
Exon 21	3694 C>T	R1232W	Missense	DIII-S1/S2	3	1, 2, 9
Exon 21	3695 G>A	R1232Q*	Missense	DIII-S1/S2	1	7
Exon 21	3716 T>C	L1239P*	Missense	DIII-S2	1	2
Exon 21	3727 G>A	D1243N*	Missense	DIII-S2	5	1, 2, 5
Exon 21	3746 T>A	V1249D*	Missense	DIII-S2	1	6
Exon 21	3758 A>G	E1253G*	Missense	DIII-S2	1	1
Exon 21	3784 G>A	G1262S	Missense	DIII-S2	1	1
Exon 21	3813 G>C	W1271C*	Missense	DIII-S3	1	1
Exon 21	3823 G>A	D1275N	Missense	DIII-S3	3	1, 5
Intron 21	3840 +1 G>A		Splice site	DIII-S3	6	1, 3, 4
Exon 22	3863 C>G	A1288G*	Missense	DIII-S3	1	4
Exon 22	3894delC	I1299SfsX13*	Frame shift	DIII-S4	1	5
Exon 22	3932 T>C	L1311P*	Missense	DIII-S4	1	7
Exon 22	3956 G>T	G1319V	Missense	DIII-S4/S5	5	2, 3, 7
Intron 22	3963 +4 A>G*		Splice site	DIII-S4/S5	1	5
Intron 22	3963 +2 T>C		Splice site	DIII-S4/S5	1	1
Exon 23	3968 T>G	V1323G*	Missense	DIII-S4/S5	1	7
Exon 23	3995 C>T	P1332L	Missense	DIII-S4/S5	1	5
Exon 23	4018 G>A	V1340I*	Missense	DIII-S5	1	9
Exon 23	4030 T>C	F1344L*	Missense	DIII-S5	1	1
Exon 23	4036 C>A	L1346I*	Missense	DIII-S5	1	4
Exon 23	4037 T>C	L1346P*	Missense	DIII-S5	1	3
Exon 23	4052 T>G	M1351R*	Missense	DIII-S5	1	2
Exon 23	4057 G>A	V1353M*	Missense	DIII-S5	2	2
Exon 23	4072 G>T	G1358W*	Missense	DIII-S5	1	4
Exon 23	4077 G>T	K1359N*	Missense	DIII-S5	1	4
Exon 23	4079 T>G	F1360C	Missense	DIII-S5/S6	1	1
Exon 23	4088 G>A	C1363Y	Missense	DIII-S5/S6	1	3

Table 4 Continued

Region	Nucleotide change	Coding effect	Mutation type	Location	No. of unrelated individuals	Testing center
Exon 23	4118 T>A	L1373X*	Nonsense	DIII-S5/S6	1	2
Exon 23	4145 G>T	S1382I	Missense	DIII-S5/S6	1	1
Exon 23	4147 C>T	Q1383X*	Nonsense	DIII-S5/S6	1	1
Exon 23	4178 T>A	L1393X	Nonsense	DIII-S5/S6	3	1, 3, 9
Exon 23	4182 C>G	Y1394X*	Nonsense	DIII-S5/S6	1	5
Exon 23	4190delA	K1397RfsX2	Frame shift	DIII-S5/S6	1	9
Exon 23	4213 G>A	V1405M*	Missense	DIII-S5/S6	2	1, 7
Exon 23	4213 G>C	V1405L	Missense	DIII-S5/S6	2	3
Exon 23	4216 G>C	G1406R	Missense	DIII-S5/S6	1	3
Exon 23	4217 G>A	G1406E*	Missense	DIII-S5/S6	2	5
Exon 23	4222 G>A	G1408R	Missense	DIII-S5/S6	7	1, 4, 5, 7
Exon 23	4226 A>G	Y1409C*	Missense	DIII-S5/S6	1	1
Exon 23	4227 C>G	Y1409X*	Nonsense	DIII-S5/S6	1	8
Exon 23	4234 C>T	L1412F*	Missense	DIII-S5/S6	1	5
Exon 24	4255 A>G	K1419E*	Missense	DIII-S5/S6	1	1
Exon 24	4258 G>C	G1420R*	Missense	DIII-S5/S6	1	3
Exon 24	4279 G>T	A1427S*	Missense	DIII-S5/S6	1	2
Exon 24	4283 C>T	A1428V*	Missense	DIII-S5/S6	1	2.
Exon 24	4294 A>G	R1432G	Missense	DIII-S5/S6	1	4
Exon 24	4296 G>C	R1432S*	Missense	DIII-S5/S6	1	2
Exon 24	4298 G>T	G1433V*	Missense	DIII-S5/S6	1	3
Exon 24	4299 G>A	G1433G*	Silent/splice site	DIII-S5/S6	1	4
Intron 24	4299 +1 G>T*		Splice site	DIII-S5/S6	1	5
Intron 24	4299 +1delG*		Splice site	DIII-S5/S6	1	1
Intron 24	4300 −1 G>A*		Splice site	DIII-S5/S6	1	2
Exon 25	4302 T>G	Y1434X*	Nonsense	DIII-S5/S6	1	5
Exon 25	4313 C>T	P1438L	Missense	DIII-S5/S6	1	4
Exon 25	4320 G>A	W1440X	Nonsense	DIII-S5/S6	1	2
Exon 25	4321 G>C	E1441Q*	Missense	DIII-S5/S6	1	7
Exon 25	4342 A>C	I1448L*	Missense	DIII-S6	1	4
Exon 25	4343 T>C	I1448T*	Missense	DIII-S6	1	2
Exon 25	4346 A>G	Y1449C*	Missense	DIII-S6	1	1
Exon 25	4352 T>A	V1451D*	Missense	DIII-S6	1	5
Exon 25	4376_4379delTCTT	F1459SfsX3*	Frame shift	DIII-S6	1	6
Exon 25	4387 A>T	N1463Y*	Missense	DIII-S6	1	2
Exon 25	4389_4396delCCTCTTTA	L1464WfsX5*	Frame shift	DIII-S6	1	8
Exon 25	4402 G>T	V1468F*	Missense	DIII-S6	1	2
Exon 25	4426 C>T	Q1476X*	Nonsense	DIII/DIV	1	4
Intron 25	4437 +5 G>A*		Splice site	DIII/DIV	2	3, 5
Exon 26	4477_4479delAAG	K1493del*	In-frame del	DIII/DIV	2	1, 7
Exon 26	4477 A>T	K1493X*	Nonsense	DIII/DIV	1	2
Exon 26	4501 C>G	L1501V	Missense	DIII/DIV	1	1
Exon 27	4562 T>A	I1521K*	Missense	DIII/DIV	1	5
Exon 27	4573 G>A	V1525M*	Missense	DIV-S1	1	4
Exon 27	4642 G>A	E1548K*	Missense	DIV-S1/S2	3	1, 4
Exon 27	4708_4710dupATC	I1570dup*	In-frame ins	DIV-S2	1	3
Exon 27	4712 T>G	F1571C*	Missense	DIV-S2	1	4
Exon 27	4720 G>A	E1574K	Missense	DIV-S2	4	2, 6, 7
Exon 27	4745 T>C	L1582P*	Missense	DIV-S2	1	3
Exon 27	4747 C>T	R1583C*	Missense	DIV-S2/S3	2	1, 2
Exon 27	4748 G>A	R1583H*	Missense	DIV-S2/S3	1	1
Exon 27	4773 G>A	W1591X*	Nonsense	DIV-S3	1	2
Exon 27	4810 G>A	V1604M*	Missense	DIV-S3	1	1
Exon 27	4813 +2_4813+5dupTGGG		Splice site	DIV-S3	1	2
Exon 28	4838 A>T	Q1613L*	Missense	DIV-S3/S4	1	1
Exon 28	4845 C>A	Y1615X*	Nonsense	DIV-S3/S4	1	2
Exon 28	4856delC	P1619RfsX12*	Frame shift	DIV-S3/S4	1	2
Exon 28	4859 C>T	T1620M	Missense	DIV-S3/S4	2	2, 9
Exon 28	4867 C>T	R1623X	Nonsense	DIV-S4	2	2, 3
Exon 28	4868 G>A	R1623Q	Missense	DIV-S4	1	5
Exon 28	4885 C>T	R1629X*	nonsense	DIV-S4	1	3
Exon 28	4886 G>A	R1629Q*	Missense	DIV-S4	1	3
Exon 28	4912 C>T	R1638X	Nonsense	DIV-S4	3	2, 3

Table 4   Continued

Region	Nucleotide change	Coding effect	Mutation type	Location	No. of unrelated individuals	Testing center
Exon 28	4925 G>A	G1642E*	Missense	DIV-S4	1	5
Exon 28	4978 A>G	I1660V	Missense	DIV-S5	5	2, 3, 5, 6
Exon 28	4981 G>A	G1661R*	Missense	DIV-S5	2	1
Exon 28	4981 G>C	G1661R*	Missense	DIV-S5	1	2
Exon 28	4999 G>A	V1667I	Missense	DIV-S5	1	3
Exon 28	5015 C>A	S1672Y	Missense	DIV-S5	2	1, 4
Exon 28	5038 G>A	A1680T	Missense	DIV-S5	2	2, 6
Exon 28	5068_5070delGA	D1690HfsX98*	Frame shift	DIV-S5/S6	1	1
Exon 28	5083 C>T	Q1695X	Nonsense	DIV-S5/S6	2	1, 4
Exon 28	5092 G>A	A1698T*	Missense	DIV-S5/S6	1	2
Exon 28	5124_5126delCAC	T1709del*	In-frame del	DIV-S5/S6	1	4
Exon 28	5126 C>T	T1709M	Missense	DIV-S5/S6	2	1, 8
Exon 28	5126 C>G	T1709R*	Missense	DIV-S5/S6	1	4
Exon 28	5134 G>A	G1712S*	Missense	DIV-S5/S6	1	7
Exon 28	5141 A>G	D1714G	Missense	DIV-S5/S6	1	3
Exon 28	5157delC	I1720SfsX67*	Frame shift	DIV-S5/S6	1	8
Exon 28	5164 A>G	N1722D*	Missense	DIV-S5/S6	1	1
Exon 28	5182 T>C	C1728R*	Missense	DIV-S5/S6	1	2
Exon 28	5184 C>G	C1728W*	Missense	DIV-S5/S6	1	2
Exon 28	5218 G>A	G1740R	Missense	DIV-S5/S6	1	3
Exon 28	5227 G>A	G1743R	Missense	DIV-S5/S6	5	4, 5, 7, 9
Exon 28	5228 G>A	G1743E	Missense	DIV-S5/S6	6	2, 3
Exon 28	5290delG	V1764SfsX23*	Frame shift	DIV-S6	1	8
Exon 28	5290 G>T	V1764F	Missense	DIV-S6	1	7
Exon 28	5336 C>T	T1779M	Missense	C-terminal	1	2
Exon 28	5350 G>A	E1784K	Missense	C-terminal	14	1, 2, 5, 6, 7
Exon 28	5356_5357delCT	L1786EfsX2*	Frame shift	C-terminal	2	1
Exon 28	5387_5388insTGA	1795_1796insD	In-frame ins	C-terminal	1	3
Exon 28	5420dupA	F1808IfsX3*	Frame shift	C-terminal	1	7
Exon 28	5435 C>A	S1812X	Nonsense	C-terminal	1	7
Exon 28	5464_5467delTCTG	E1823HfsX10*	Frame shift	C-terminal	1	2
Exon 28	5494 C>G	Q1832E*	Missense	C-terminal	1	6
Exon 28	5577_5578dupAA	R1860KfsX13*	Frame shift	C-terminal	1	2
Exon 28	5581 G>A	V1861I*	Missense	C-terminal	1	2
Exon 28	5616 G>C	K1872N*	Missense	C-terminal	1	5
Exon 28	5707 G>C	S1904L	Missense	C-terminal	1	2
Exon 28	5770 G>A	A1924T	Missense	C-terminal	1	3
Exon 28	5803 G>A	G1935S	Missense	C-terminal	1	2
Exon 28	5812 G>A	E1938K*	Missense	C-terminal	1	2
Exon 28	6010_6012dupTTC	F2004dup*	In-frame ins	C-terminal	1	7
Exon 28	6010 T>G	F2004V*	Missense	C-terminal	1	5

del = deletion; dup = duplication; ins = insertion; indel = insertion/deletion; ins = insertion; * = novel mutation; Testing Center: 1 = Nantes; 2 = Brugada; 3 = AMC; 4 = Paris; 5 = PGxHealth; 6 = MMRL; 7 = UKM; 8 = NCVC; 9 = BCM.

significant loss of sodium channel function through a mechanism of haploinsufficiency. Recently, Meregalli et al[29] reported that BrS patients with truncation mutations, caused by radical mutations, had a more severe phenotype characterized as a higher propensity for syncope and prevalence of SCD among young first-degree relatives, than those BrS patients hosting missense mutations functionally characterized with ≤90% peak sodium current reduction.

The SCN5A-encoded cardiac voltage-gated sodium channel (Nav1.5), which is responsible for the initial fast upstroke of the cardiac action potential and accordingly plays a vital role in the excitability of myocardial cells and the proper conduction of the electrical pulsation of the heart, consists of 4 homologous domains (DI-DIV) that are connected by intracellular linkers. Each domain contains 6 transmembrane-spanning seg-

ments (S1-S6). Although case mutations were scattered throughout Nav1.5, there was clustering of putative BrS1-associated mutations whereby nearly three-fourths localized to the transmembrane and pore-forming domains compared with <20% of the rare variants found among the control subjects. Further, nearly 10% of patients with clinically suspected BrS had a mutation localizing to the channel's pore/selectivity filter (segments S5 and S6 and the interconnecting P-loops) compared with <0.5% of the control subjects. Because of the extreme rarity of pore-localizing missense variants among the healthy control subjects, such missense mutations found in cases are high probability BrS1-causative mutations. However, whether BrS1 patients with pore mutations behaved more poorly than those with mutations localizing to other domains was unable to be gleaned in this study.
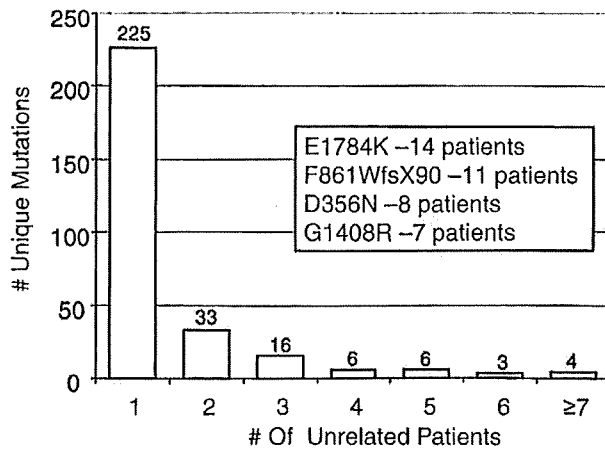
Figure 2 BrS1-associated mutation frequency distribution. This bar graph summarizes the distribution of specific mutations among unrelated patients. The Y-axis depicts the number of unique BrS1-associated mutations, and the X-axis represents the number of unrelated patients. For example, the first column indicates that there were 226 unique mutations each observed only once. The last column indicates that 4 different BrS1-associated mutations were each seen in ≥7 unrelated patients. The inset shows the 4 most common BrS1-associated mutations identified and the number of specified unrelated patients in whom the mutations were found.

In contrast, only 25 patients hosted a single missense mutation residing in either the DI-DII or DII-DIII linker domains. The observed preponderance (over 50% of which localize to these 2 IDLs) of the 42 unique rare missense variants identified in the healthy control subjects suggest that some of the 21 IDL localizing, possible BrS1-associated missense mutations that were identified in 25 cases may in fact represent false positives.[11,13] Despite being absent in over 1,300 control subjects, either cosegregation or functional studies on these DI-DII and DII-DIII linker-localizing mutations should be considered before upgrading their status from a rare variant of uncertain significance to a probable BrS1-causative missense mutation. For example, 1 of the 21 missense mutations, G615E, has been previously characterized as having no significant changes in current density or kinetics compared with wild type, casting some doubt on its level of causality.[25]

Whereas loss-of-function mutations in SCN5A have been shown to serve as a pathogenic basis for BrS, gain-of-function mutations in SCN5A provide the pathogenic substrate for LQT3, a clinically and mechanistically distinct arrhythmia syndrome from BrS. Interestingly, 10 mutations identified in this BrS compendium have been implicated previously in LQTS, including the most commonly observed mutation, E1784K. In fact, E1784K represented the most commonly observed SCN5A mutation (4/26, ~15%) among a cohort of 541 unrelated LQTS patients.[28] Although the clinical phenotype for the patients hosting 1 of these 10 mutations could have been assigned incorrectly, it is far more likely that these represent overlap syndrome/mixed phenotype syndrome–associated SCN5A mutations.

For example, E1784K represents the quintessential example of a cardiac sodium channel mutation with the capacity to provide for a mixed clinical phenotype of LQT3, BrS, and conduction disorders.[30] Makita et al[30] reported recently a high prevalence of LQT3/BrS/conduction phenotype overlap among 41 E1784K carriers from 15 kindreds of diverse ethnic background. Of the 41 cases, 93% displayed a prolonged QTc, 22% with a diagnostic indicator (ST-segment elevation or positive provocation test) of BrS, and 39% had sinus node dysfunction. Functional characterization of mutant E1784K sodium channels displayed unique biophysical and pharmacological properties consistent with other mutations that yield a mixed phenotype, including a negative shift of steady-state sodium channel activation and enhanced tonic block in response to sodium channel blockers, leading to an additional BrS/sinus node dysfunction phenotype in conjunction with a prolonged QTc.[30] This particular functional effect may influence the pharmacological management of patients with E1784K-SCN5A disease.[30]

Similarly, Bezzina et al[31] in 1999, described an LQT3/BrS overlap phenotype in a large 1795insD-SCN5A mutation–positive 8-generation kindred characterized with a high incidence of sudden nocturnal death, QT-interval prolongation, and Brugada ECG. Whether or not the 9 other mutations, identified here in BrS patients and elsewhere in patients purported to have LQTS, have a similar functional characteristic that provides a substrate for producing a mixed/overlapping clinical phenotype remains to be seen.

Given that SCN5A remains the most common BrS genotype despite accounting for only 20% of BrS, genetic heterogeneity of the disease is evident and the role of genetic background in the pathophysiology of BrS is important.[32] Recently, mutations in the glycerol-3-phosphate dehydrogenase 1–like protein encoded by GPD1L have been shown to affect trafficking of the sodium channel to the plasma membrane, thus reducing overall sodium current, giving rise to the BrS phenotype.[33] Recently, mutations involving the L-type calcium channel alpha and beta subunits encoded by the CACNA1C and CACNB2b genes,
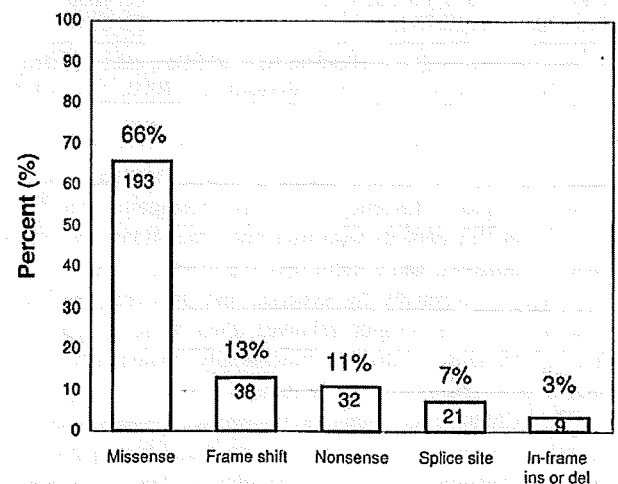

Figure 3 Summary of SCN5A mutation type for BrS1. The distribution of mutation type (missense, frameshift, etc.) is summarized for the possible BrS1-associated SCN5A mutations. The number within the column represents the total number of unique mutations for the respective type. For example, there were 193 unique missense mutations identified.